Heliyon 10 (2024) e35126

Contents lists available at ScienceDirect

Heliyon

journal homepage: www.cell.com/heliyon

Research article

Methylome analysis of endothelial cells suggests new insights on sporadic brain arteriovenous malformation

Concetta Scimone [a,b], Luigi Donato [a,b], Simona Alibrandi [a,b,*], Alfredo Conti [c,d], Carlo Bortolotti [c], Antonino Germanò [e], Concetta Alafaci [e], Sergio Lucio Vinci [f], Rosalia D'Angelo [a,b], Antonina Sidoti [a,b]

[a] *Department of Biomedical and Dental Sciences and Morphofunctional Imaging, University of Messina, Via Consolare Valeria 1, 98125, Messina, Italy*
[b] *Department of Biomolecular Strategies, Genetics, Cutting-edge Therapies, I.E.ME.S.T., Via Michele Miraglia 20, Palermo, 90139, Italy*
[c] *IRCCS Istituto Delle Scienze Neurologiche di Bologna, Bologna, Via Altura 3, 40123, Bologna, Italy*
[d] *Department of Biomedical and NeuroMotor Sciences (DiBiNeM), Alma Mater Studiorum – University of Bologna, Bologna, Italy*
[e] *Neurosurgery Unit, Department of Biomedical and Dental Sciences and Morphofunctional Imaging, University of Messina, Via Consolare Valeria 1, 98125, Messina, Italy*
[f] *Neuroradiology Unit, Department of Biomedical and Dental Sciences and Morphofunctional Imaging, University of Messina, Messina, Italy*

ARTICLE INFO

Keywords:
Brain arteriovenous malformation
Mural cells
Epigenetics
Transcription factors

ABSTRACT

Arteriovenous malformation of the brain (bAVM) is a vascular phenotype related to brain defective angiogenesis. Involved vessels show impaired expression of vascular differentiation markers resulting in the arteriolar to venule direct shunt. In order to clarify aberrant gene expression occurring in bAVM, here we describe results obtained by methylome analysis performed on endothelial cells (ECs) isolated from bAVM specimens, compared to human cerebral microvascular ECs. Results were validated by quantitative methylation-specific PCR and quantitative realtime-PCR. Differential methylation events occur in genes already linked to bAVM onset, as *RBPJ* and *KRAS*. However, among differentially methylated genes, we identified *EPHB1* and several other loci involved in EC adhesion as well as in EC/vascular smooth muscle cell (VSMC) crosstalk, suggesting that only endothelial dysfunction might not be sufficient to trigger the bAVM phenotype. Moreover, aberrant methylation pattern was reported for many lncRNA genes targeting transcription factors expressed during neurovascular development. Among these, the YBX1 that was recently shown to target the arteridin coding gene. Finally, in addition to the conventional CpG methylation, we further considered the role of impaired CHG methylation, mainly occurring in brain at embryo stage. We showed as differentially CHG methylated genes are clustered in pathways related to EC homeostasis, as well as to VSMC-EC crosstalk, suggesting as impairment of this interaction plays a prominent role in loss of vascular differentiation, in bAVM phenotype.

* Corresponding author. Department of Biomedical and Dental Sciences and Morphofunctional Imaging, University of Messina, Via Consolare Valeria 1, 98125, Messina, Italy.
E-mail address: salibrandi@unime.it (S. Alibrandi).

https://doi.org/10.1016/j.heliyon.2024.e35126
Received 5 July 2024; Accepted 23 July 2024
Available online 30 July 2024

1. Introduction

Epigenetic events lead differential gene expression during both development and adulthood. Since these modifications don't alter DNA sequence, their involvement in phenotype determination was recently considered. Epigenetics includes covalent reversible modifications as acetylation and methylation. In particular, methylation can occur on cytosine (C) residues, resulting in gene silencing. In detail, target cytosines are most often located within the CpG islands distributed along promoters, regulatory regions and intron-exon boundaries [1]. However, non-CpG methylation can occur involving the C of the CHG trinucleotide, where H is A, T or C. CHG methylation was initially discovered in plants [2]. In humans, CHG methylation plays an essential role during development and it is active in embryo and in pluripotent stem cells [3]. In adulthood, instead, CHG methylation is the main methylation kind occurring in brain [4]. Furthermore, brain CHG hypomethylated genes were also clustered in the "blood vessel development" GeneOntology biological process [5], suggesting that epigenetics tightly controls brain microvasculature development during capillary tube formation [6]. Among congenital vessel malformations, arteriovenous malformation of the brain (bAVM, OMIM #108010) onsets following impaired expression of genes involved in vascular differentiation and, most likely, during late angiogenesis and arterialization. Brain AVM is featured by the direct arteriole-to-venule shunt. As consequence, absence of the capillary bed results in the high pressure blood perfusion through the lesion nidus, making it prone to rupture. For this reason, bAVM is classified as high-flow lesion and its clinical manifestation most often culminates with stroke and seizure. Moreover, bAVM vessels undergo to continuous remodelling phenomena involving both affected and neighbour arterioles [7]. Central and peripheral AVMs can coexist with telangiectasias, in the inherited Osler-Weber-Rendu disease, also known as hereditary haemorrhagic telangiectasia (HHT). This condition arises following germline mutations in the *ACVRL1*, *ENG*, *SMAD4*, *GDF2* and *BMP9* genes Drapè et al., 2022, encoding for TGFBR2/BMP signalling related proteins. On the other hand, knowledge about developmental dysfunction resulting in sporadic bAVM is still very elusive. Vascular differentiation markers are expressed early during embryogenesis, when vessel identity begin to be established. In this context, the erythropoietin-producing hepatocellular carcinoma (Eph) receptors and their ligands ephrins play a pivotal role. Briefly, the primitive capillary plexus co-expresses both ephrin B2 (*EFNB2* gene) and EphB4 (*EPHB4* gene), despite they become differential markers for arterial and venous endothelia, respectively [8,9]. Upstream, differential ephrin B2/EphB4 expression is driven by VEGFA/VEGFR2-induced Notch signalling [10]. Several further pathways contribute to the correct arteriovenous specification and their perturbation most likely results in bAVM phenotype (Table 1). Moreover, studies performed on bAVM specimens confirmed the amplification of the Sonic Hedgehog (Shh) pathway [11], as well as the high incidence of *KRAS* gain of function G12V missense mutation in pathological tissues [12]. Taken together, these findings suggest the complexity of mechanisms involved in vessel specialization, making the cause of congenital bAVM very challenging to decipher. In order to further characterize aberrant gene expression in bAVM pathogenesis, we obtained the methylome profile of ECs isolated from bAVM specimen, finding that impaired methylation occurs in novel gene sets involved in both vascular differentiation and in vascular smooth cell (VSMC)/EC interaction. Moreover, our data further suggest as aberrant CHG methylation in genes related to neurovascular development may contribute to bAVM phenotype.

2. Results

2.1. EC purity assessment

Quantification of both endothelial cell (EC) and VSMC markers was performed by qRT-PCR. Expression values were compared between bAVM tissues and HCMECs. In detail, *CDH5* and *PECAM1* were considered as endothelial markers, while *DES* and *MYH11* as markers for VSMCs. Quantitative RT-PCR data confirmed purity of EC isolation procedure, as shown in Fig. 1. In detail, expression profile comparison between bAVM-derived ECs and HCMECs showed no significant differences for the *CDH5* marker. About *PECAM1*, its expression resulted increased in bAVM ECs. Interestingly, expression of both VSMC markers *MYH11* and *DES* was comparable between bAVM purified ECs and HCMECs, confirming purity of purification process.

Table 1
Loci associated to bAVM development.Key genes related to bAVM pathogenesis are listed in the second column (target gene). Upstream and downstream refer to genes acting by regulating target gene expression and regulated by target genes, respectively. ↓: downexpression; ↑: overexpression.

Upstream gene	Target gene	Downstream gene	Biological process	Reference
SOX17	*NOTCH4*	*CXCR4*, *HEY1*, *DLL4*, *DLL1*	Arterial specification	[13]
	CDX2	*HOX-A* gene cluster	Arterial specification	[14]
↓ ***SOX7/SOX8***	↓ Ephrin B2 ↓ Gridlock		Arterial differentiation loss	[15]
↑ ***SOX2***	↑ Notch-Skip axis		bAVM-like phenotype	[16]
RBPJ	*NOTCH4/HES1* signalling		bAVM-like phenotype	[17]
	SOX2		Endothelial-to-mesenchymal transition (EndMT)	[18]
RASA1 loss of function	*KLF2A*	MEK/ERK signalling	Vein differentiation loss	[19,20]

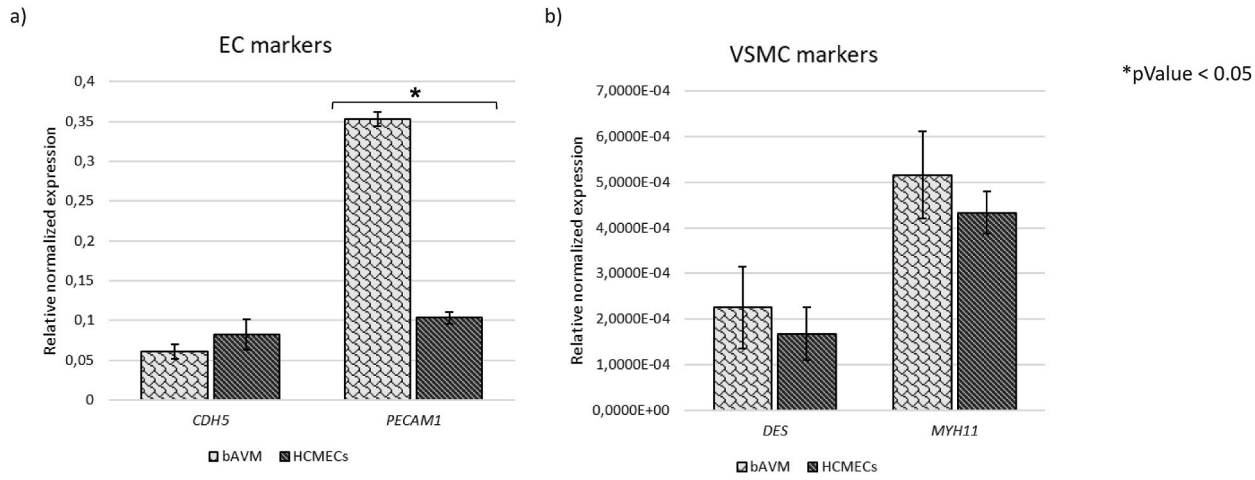

Fig. 1. EC purity evaluation. Expression of endothelial cell markers in purified bAVM ECs were evaluated by quantitative RT-PCR. *CDH5* and *PECAM1* were considered to test endothelial identity. *DES* and *MYH11* expression was quantified in order to evaluate VSMC contamination. No differences were observed about VSMC markers between bAVM ECs and HCMECs. PECAM1, instead, resulted overexpressed in bAVM ECs, suggesting EC identity. Its overexpression when compared to HCMECs is related to the pathological phenotype. *Bonferroni-adjusted pValue.

2.2. Sequencing output

Sequencing of bisulfite-converted DNA generated 1,488,651,512 and 1,248,902,540 reads for bAVM and HCMEC samples, respectively (SM1). Of these, 99.86 % and 99.75 % were uniquely mapped against the GRCh38 Human Reference Genome. About Metilene tool, 639 CHG sites and 27689 CpG islands resulted differentially methylated between bAVM ECs and HCMECs, spanning along 589 and 11653 loci (SM2). In detail, 490 loci are interested by both modification kinds (Fig. 2a) (SM3). Hypomethylation was more represented and, according to chromosomal distribution, chromosome 2 is the most affected by both CpG and CHG aberrant modifications (Fig. 2b). As shown in Fig. 3, differential methylation events most often occur in noncoding regions.

2.3. Methylation status of coding genes involved in bAVM related pathways

As first observation, methylation rate of genes involved in bAVM development was evaluated. Increase of normal methylation rate was observed for *RASA1*, *RBPJ* and *SOX7*, while CpG islands regulating *SHH* expression were hypomethylated. Then, all differentially methylated coding genes were selected and enriched, resulting clustered in 125 pathways related to cell adhesion, cation transport, neuronal development and vascular development (SM4). In detail, this last cluster includes pathways as “VEGF signalling”, “PDGF signalling”, “EPHB pathway”, “BMP signalling”, “PAR-mediated signalling”, “S1P1 pathway” and “Signalling events mediated by the Hedgehog family” (Fig. 4a). Genes clustered in these signalling cascades comprise *EPHB1* and *EFNA5* that are known to induce vascular specialization and remodelling [21]. Moreover, the SHH receptor coding genes *CDON* and *GAS1* resulted hypermethylated, while the transcription factors *GLI2* and *GLI3* resulted hypomethylated, when compared to the HCMEC methylation profile. Moreover, several genes clustered in “VEGF-PDGF signalling” were enriched in other bAVM related pathways (Fig. 4b) (Table 2) (SM4).

2.4. Differentially methylated genes involved in cell-cell and cell-extracellular matrix adhesion

Proteins of the extracellular matrix (ECM) surrounding ECs are crucial for angiogenesis and vascular remodelling [28] and, in this context, several genes involved in EC-ECM adhesion resulted differentially methylated, when compared to HCMEC methylation profile (SM4) (Table 2). In detail, TGF-β related genes (*TGFBI*, *ITGA8*, *PARVA* and *PARD3*) resulted hypomethylated, suggesting the amplification of this cascade signalling. However, evidence of TGFB1 pathway in extracranial AVM has been already reported [29]. Likewise, the integrin-mediated cell adhesion pathway was enriched with genes that take part to vascular specialization as *ADAM12* Wang et al., 2023, *COL4A1* (Kumar et., 2022), *SLIT2* [30], *VCAM1* [31]. Finally, genes clustered in both canonical and non-canonical Wnt pathways include the hypomethylated *FZD7*, *WNT7B*, *CHD7* and the hypermethylated *FZD10*, *RYK*, *DAAM1*, *ROR2*.

2.5. Enrichment analysis of differentially methylated noncoding genes

Among noncoding genes, differential methylation events mostly affect lncRNA ones (Fig. 3a) (SM2). According to their biological role, *GAS5*, *PVT1*, *SNHG15*, *CASC11*, *SOX2-OT*, *FENDRR* were prioritized. In detail, *GAS5*, *PVT1* and *CASC11* showed a hypomethylation pattern, while *FENDRR*, *SOX2-OT* and *SNHG15* were hypermethylated (Table 2). By the RNAInter interactome repository, target genes of differentially methylated noncoding RNAs were identified and these mostly include pseudogenes and transcription factors (Fig. 5a) (SM5). Also in this case, they were enriched in pathways related to VEGF, PDGF, Notch, Wnt and integrin signalling

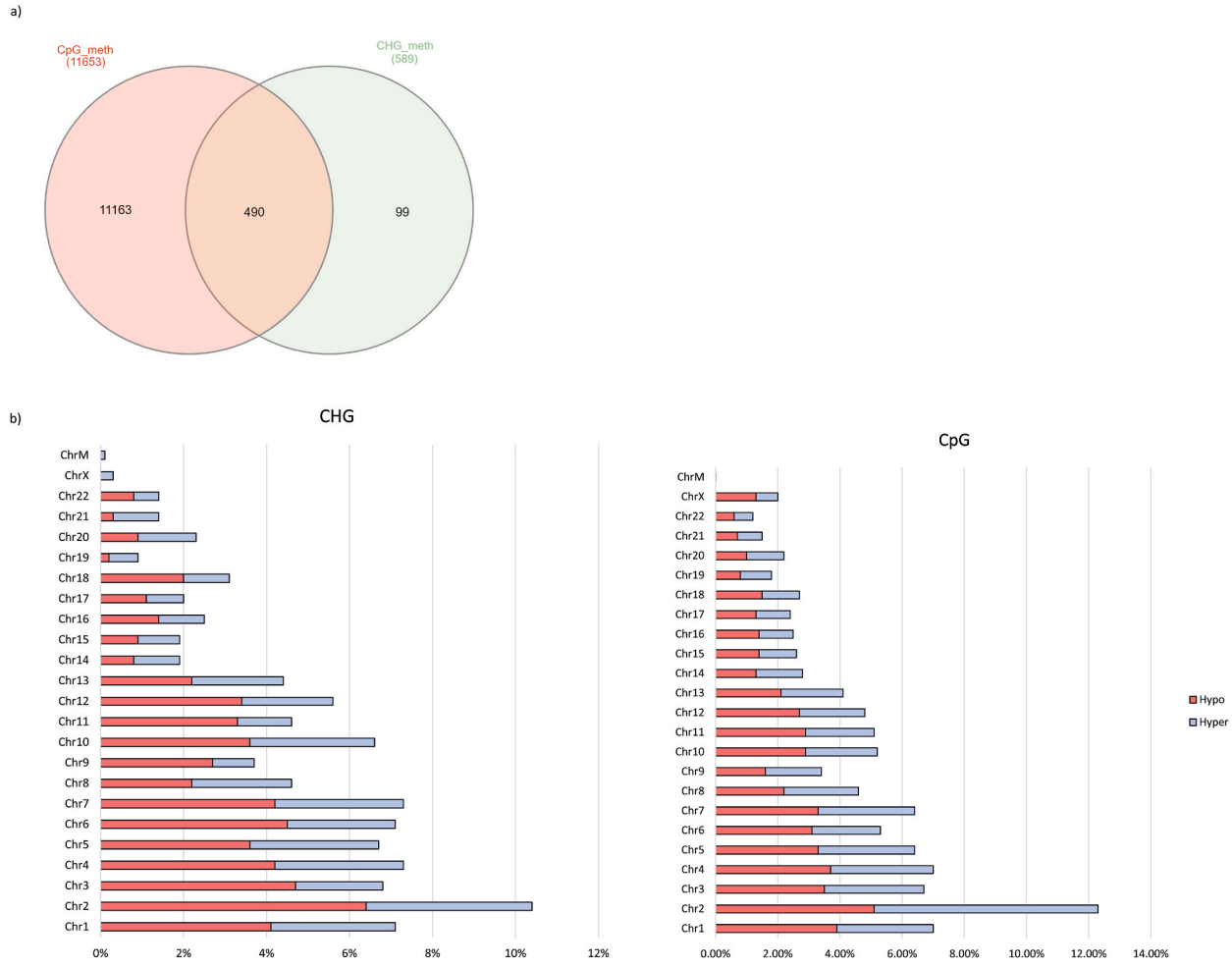

Fig. 2. Differentially methylated sites. a) Differentially methylated genes, according to the CpG or CHG sites. As shown, 490 loci are interested by both CpG and CHG differential methylation. b) Chromosome distribution of differentially methylated loci. For each chromosome, the percentage of differentially methylated genes is calculated against the total differentially methylated gene number. Red: hypomethylated loci. Blue: hypermethylated loci.

(Fig. 5b). Interestingly, several ncRNAs were found to target the same transcription factors (Fig. 5c). Of these, several were already described in bAVM pathogenesis (*SOX2*, *KLF4*, *KLF5*, *SPI1*, *SMAD2*, *RUNX1*, *SMAD3*, *CDX2*). However, *EZH2*, *TAL1*, *YBX1*, *QKI*, *FOXM1*, *EOMES*, *SNAI1*, *ELAVL1*, *RBFOX2*, *ERG* were here considered, according to their involvement in cell-ECM adhesion that regulates vascular differentiation and vascular smooth muscle cell (VSMC) physiology [29,14,32–41], Zhang et al., 2022, Jia et al., 2023. As genes targeted by the differentially methylated noncoding RNAs but not yet associated to the phenotype (Table 3), their possible dysregulation in bAVM ECs was evaluated by qRT-PCR. Interestingly, impairment of their expression pattern was confirmed (Fig. 6). In detail, *TAL1*, *YBX1*, *QKI*, *ELAVL1* and *SNAI1* resulted upregulated, while *EZH2*, *ERG* and *RBFOX2* were down-expressed when compared to HCMECs. Moreover, methylation profile of most of these genes does not differ between bAVM ECs and HCMECs, supporting the hypothesis that their expression can be impaired due to aberrant methylation of the targeting noncoding RNAs. No significant difference was observed for *EOMES* and *FOXM1* expression. Taken together, these data suggest that impaired expression of vessel differentiation markers could not be the only mechanism responsible for defective arteriovenous shunt but also other factors, as the aberrant cross-talk between ECs and VSMCs, may contribute to the AVM phenotype.

2.6. Methylation profile validation

In order to confirm data obtained by the methylome sequencing, methylation of CpG islands of 7 coding genes and 5 noncoding genes was evaluated by quantitative methylation-specific PCR (qMSP). Fig. 7 summarizes results obtained by 11 bAVM samples, expressed as percent methylated reference (PMR). Differential methylation was confirmed for all considered loci, with the exception of *FZD10*, resulted hypomethylated.

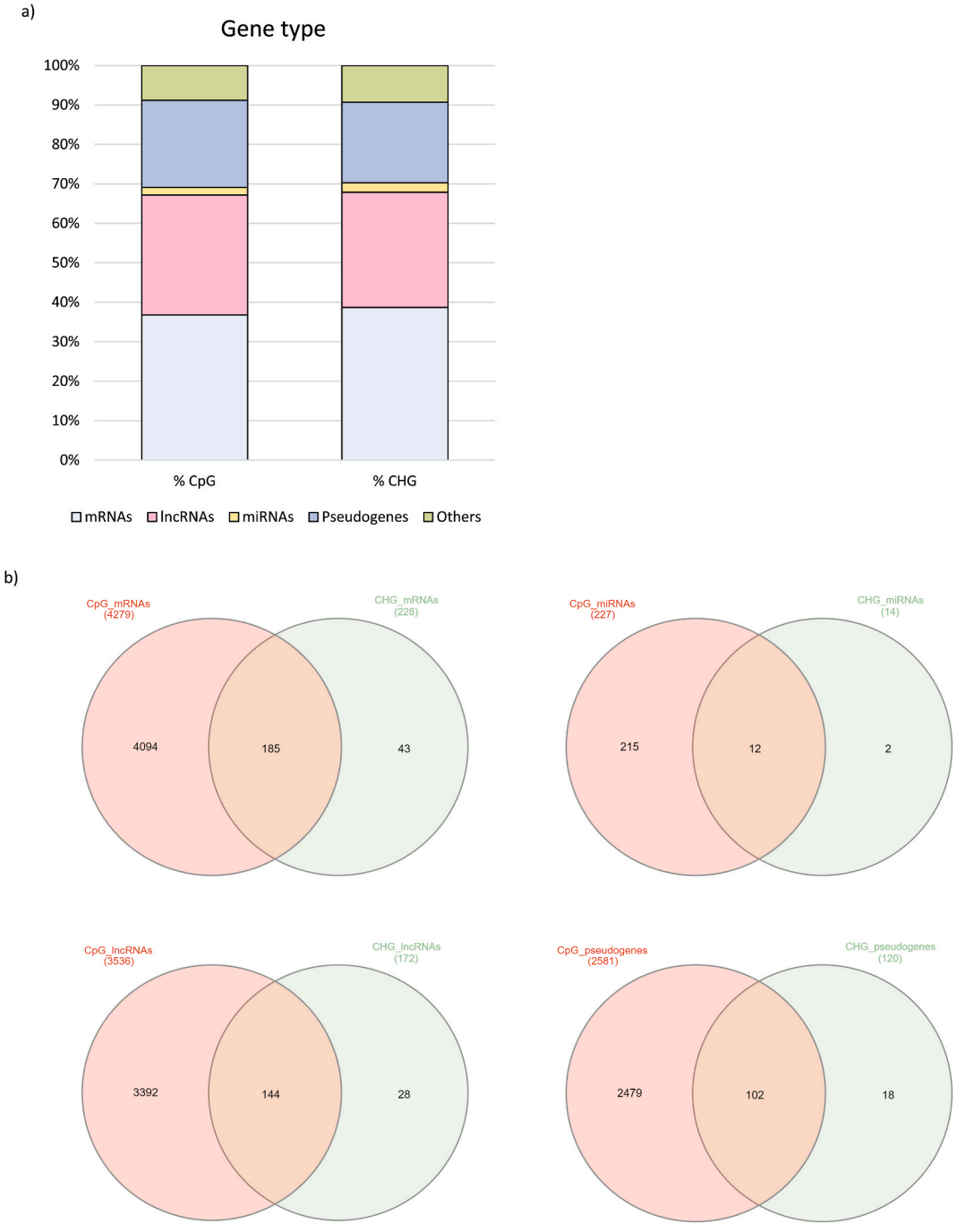

Fig. 3. Differential methylation events in gene biotypes. a) Bar chart showing as each modification (CpG or CHG) affects the different gene biotypes. Both CpG and CHG aberrant methylation mostly occurs in noncoding genes. b) For each biotype, number of genes interested by differential CpG or CHG modifications is shown.

2.7. Role of CHG methylation

CHG methylation is a non-CpG epigenetic regulation occurring during embryo development and involved in CNS vessel remodelling in adulthood [5]. Also CHG differential methylation mainly occurs in noncoding genes in bAVM sample (Fig. 3a). Moreover, among mRNA coding genes, only 43 are uniquely interested by CHG methylation (Fig. 3b) (SM3). According to their involvement in vascular development and their expression pattern during development and in adulthood, *CERS2*, *NRP1*, *TBX18*, *GAPVD1* and *SALL4* were selected to be validated by qRT-PCR (Table 4) (Fig. 8), confirming their altered methylation profile.

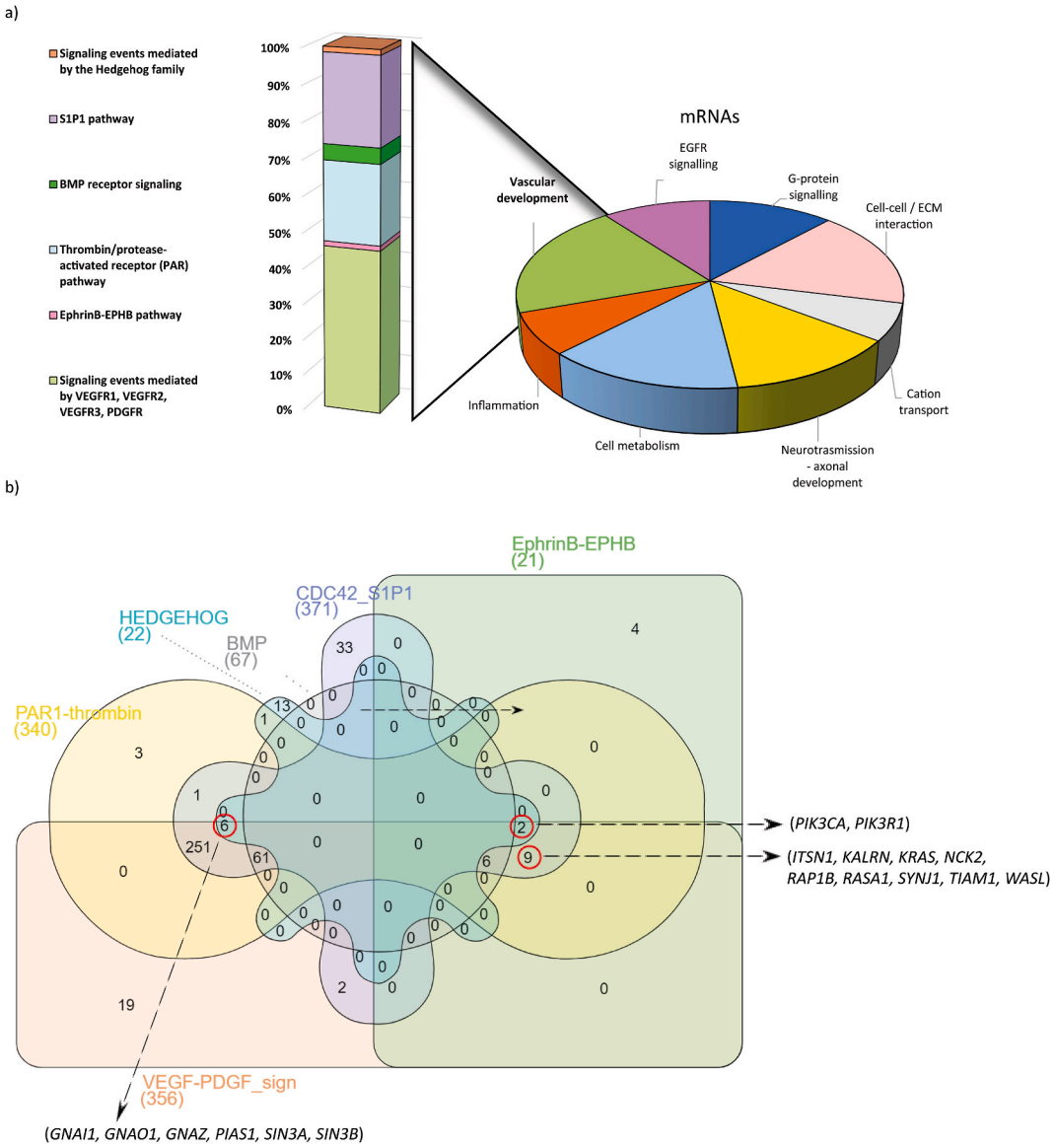

Fig. 4. Pathway analysis for coding genes. a) Pathways enriched by differentially methylated genes. About vascular development, aberrant methylation mostly occurs in genes involved in VEGF signalling. b) Differentially methylated genes enriched in different angiogenesis-related pathways. Red circles indicate the prioritized loci. In detail, *PIK3CA* and *PIK3R1* are common to all considered pathway with the exception of "BMP" one; *ITSN1*, *KALRN*, *KRAS*, *NCK2*, *RAP1B*, *RASA1*, *SYNJ1*, *TIAM1* and *WASL* are common to "VEGF", "Ephrin", "CDCD42" and "PAR1" signalling; *GNAI1*, *GNAO1*, *GNAZ*, *PIAS1*, *SIN3A*, *SIN3B* are shared by the "VEGF", "SHH", "CDCD42" and "PAR1" pathways.

2.8. *KRAS somatic mutations*

By direct sequencing of *KRAS* coding regions, 2 heterozygous variants were detected in 2 different sporadic patients. The rs1137282 (Fig. 9a) is a synonymous substitution (c.519 T > C, p.Asp173Asp; Minor Allele Frequency = 0.2173) reported in the COSMIC database (https://cancer.sanger.ac.uk/cosmic, Id: COSV55562336) having been it identified in meningioma, thyroid and large intestine carcinoma tissues and leukemia cells. Likewise, the rs12313763 (c.451-9G > A) is an intronic variant occurring 9 nucleotides upstream of the spice site of the 5th exon (Fig. 9b). Its frequency is about 0.01761 worldwide and, also in this case, it is described in the COSMIC database (COSV55527560) as recurrent mutation in large intestine and prostate cancers. Moreover, it was also detected in haemangioblastoma cells. As expected, neither the rs1137282 nor the rs12313763 were detected in the germline DNA of the same patients. These data further confirm the existence of somatic *KRAS* variants in sporadic bAVM ECs.

Table 2
Prioritized loci. Among differentially methylated genes, several were prioritized as likely related to bAVM onset. For each gene, chromosomal locus (I column), name and HGNC Id (II column), gene biotype (III column), methylation status (IV column), biological pathways (V column), evidence of involvement in bAVM pathogenesis (VI column) are reported. HGNC: Human Genome Nomenclature Committee.

Locus	Gene (HGNC Id)	Gene biotype	Methylation status	GO Biological process related to bAVM pathogenesis	Involvement in bAVM pathogenesis
1q25.1	*GAS5 (16355)*	RNA gene	Hypo	(GO:0034599) cellular response to oxidative stress	Not reported
1p21.2	*VCAM1 (12663)*	Protein coding	Hypo	(GO:0035924) cellular response to vascular endothelial growth factor stimulus, (GO:0007160) cell-matrix adhesion, (GO:0001666) response to hypoxia	[22]
2q14.2	*GLI2 (4318)*	Protein coding	Hypo	(GO:0007224) smoothened signalling pathway,	Not reported
2q33.1	*FZD7 (4045)*	Protein coding	Hypo	(GO:0060071) Wnt signalling pathway, planar cell polarity pathway	Not reported
3q22.2	*RYK (10481)*	Protein coding	Hyper	(GO:0035567) non-canonical Wnt signalling pathway	Not reported
3q22.2	*EPHB1 (3392)*	Protein coding	Hyper	Angiogenesis (GO:0001525), cell adhesion (GO:0007155	Not reported
3q26.32	*PIK3CA (8975)*	Protein coding	Hypo	(GO:0001944) vasculature development, (GO:0048661) positive regulation of smooth muscle cell proliferation,	Not reported
3q26.33	*SOX2-OT (20209)*		Hyper		Not reported
4p15.2	*RBPJ (5724)*	Protein coding	Hyper	Angiogenesis (GO: 0001525), blood vessel remodelling (GO: 0001974), artery morphogenesis (GO:0048844)	[23]
4p15.31	*SLIT2 (11086)*	Protein coding	Hypo	(GO:0002042) cell migration involved in sprouting angiogenesis, (GO:0010596) negative regulation of endothelial cell migration,	Not reported
5q13.1	*PIK3R1 (8979)*	Protein coding	Hyper	(GO:0001953) negative regulation of cell-matrix adhesion, (GO:0051491) positive regulation of filopodium assembly	Not reported
5q14.3	*EDIL3 (3173)*	Protein coding	Hyper	(GO:0007155) cell adhesion	[24]
5q14.3	*RASA1 (9871)*	Protein coding	Hyper	(GO:0001570) vasculogenesis, (GO:0030833) regulation of actin filament polymerization	[20]
5q21.3	*EFNA5 (3225)*	Protein coding	Hypo	(GO:0022407) regulation of cell-cell adhesion	Not reported
6q21	*LAMA4 (6484)*	Protein coding	Hyper	(GO:0001568) blood vessel development, (GO:0030155) regulation of cell adhesion	[25]
7q36.3	*SHH (10848)*	Protein coding	Hypo	(GO:0001569) branching involved in blood vessel morphogenesis, (GO:0002320) lymphoid progenitor cell differentiation, (GO:0060840) artery development,	[11]
7p13	*SNHG15 (27797)*	RNA gene	Hyper	(GO:0006396) RNA processing	Not reported
7p14.1	*GLI3 (4319)*	Protein coding	Hyper	(GO:0045879) negative regulation of smoothened signalling pathway, (GO:0060840) artery development,	Not reported
8q12.2	*CHD7 (20626)*	Protein coding	Hypo	(GO:0001568) blood vessel development, (GO:0001974) blood vessel remodelling, (GO:0048844) artery morphogenesis	Not reported
8q24.21	*CASC11 (48939)*	RNA gene	Hypo	Not reported	Not reported
8q24.21	*PVT1 (9709)*	Protein coding	Hypo	(GO:0010628) positive regulation of gene expression	Not reported
8p23.1	*SOX7 (18196)*	Protein coding	Hyper	Regulation of canonical Wnt signalling pathway (GO:0060828)	[15]
9q21.33	*GAS1 (4165)*	Protein coding	Hyper	(GO:0008589) regulation of smoothened signalling pathway, (GO:0035924) cellular response to vascular endothelial growth factor stimulus,	Not reported
9q22.31	*ROR2 (10257)*	Protein coding	Hyper	(GO:0060071) Wnt signalling pathway, planar cell polarity pathway	Not reported
10q26.2	*ADAM12 (190)*	Protein coding	Hypo	(GO:0045766) positive regulation of angiogenesis, (GO:0007229) integrin-mediated signalling pathway	Not reported
11q24.2	*CDON (17104)*	Protein coding	Hyper	(GO:0007224) smoothened signalling pathway	Not reported
12q24.33	*FZD10 (4039)*	Protein coding	Hyper	(GO:0035567) non-canonical Wnt signalling pathway	Not reported
12p12.1	*KRAS (6407)*	Protein coding	Hypo		[26], [27]
13q34	*COL4A1 (2202)*	Protein coding	Hypo	(GO:0001569) branching involved in blood vessel morphogenesis	Not reported
14q23.1	*DAAM1 (18142)*	Protein coding	Hyper	(GO:0060071) Wnt signalling pathway, planar cell polarity pathway	Not reported
16q24.1	*FENDRR (43894)*	RNA gene	Hyper	Not reported	Not reported

(*continued on next page*)

Table 2 (*continued*)

Locus	Gene (HGNC Id)	Gene biotype	Methylation status	GO Biological process related to bAVM pathogenesis	Involvement in bAVM pathogenesis
22q13.31	*WNT7B (12787)*	Protein coding	Hypo	(GO:0022009) central nervous system vasculogenesis, (GO:0016055) Wnt signalling pathway	Not reported

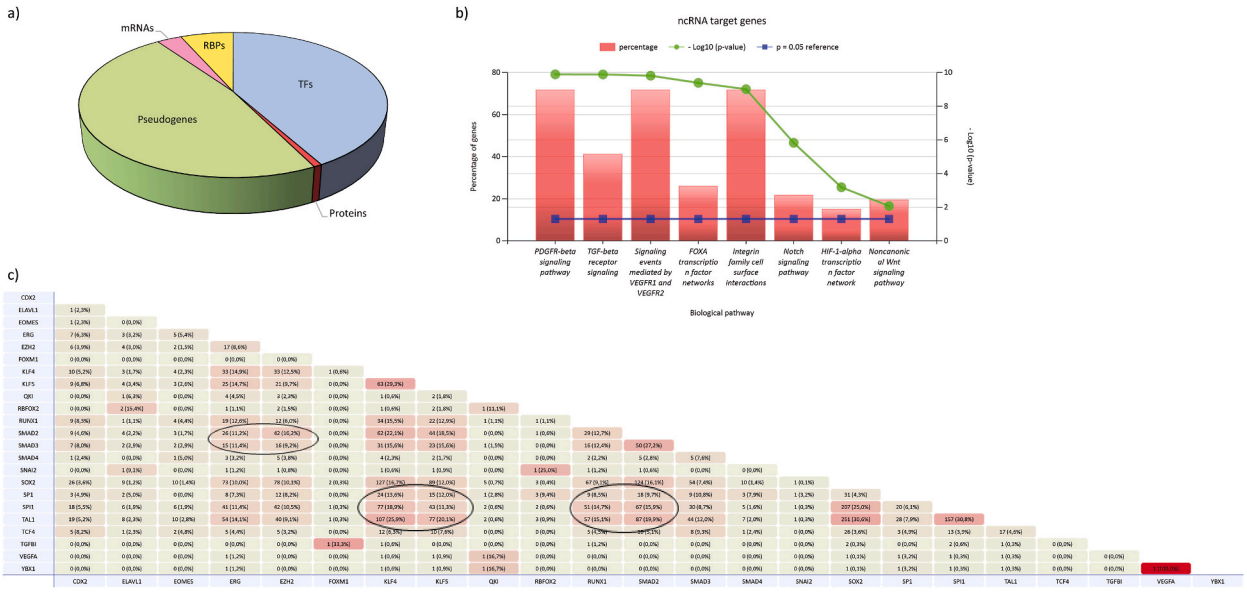

Fig. 5. Gene biotypes targeted by differentially methylated noncoding genes. a) Pie chart showing as most of genes targeted by differentially methylated noncoding RNAs include pseudogenes and transcription factors. b) Pathways enriched by genes targeted by the differentially methylated noncoding RNAs. They include signalling related to angiogenesis, to ECM signalling and VSMC homeostasis. c) For each gene-pair, percentage of differentially methylated noncoding genes targeting them is reported.

Table 3
Transcription factors targeted by differentially methylated noncoding genes. Chromosomal locus, gene name and HGCN Id, biological processes and literature data suggesting their possible involvement in bAVM pathogenesis are reported.

Locus	Gene (HGNC Id)	GO Biological process related to bAVM pathogenesis	Involvement in bAVM pathogenesis
1p33	*TAL1*	(GO:0001525) angiogenesis, (GO:0035162) embryonic hemopoiesis, (GO:0060217) hemangioblast cell differentiation	[42]
1p34.1	*YBX1 (8014)*	(GO:0006397) mRNA processing	[43] , [44]
3p24.1	*EOMES (3372)*	(GO:0048382) mesendoderm development, (GO:0010002) cardioblast differentiation	[39]
6q26	*QKI (21100)*	(GO:0001570) vasculogenesis, (GO:0035886) vascular associated smooth muscle cell differentiation	[45]
7q36.1	*EZH2 (3527)*	(GO:0010718) positive regulation of epithelial to mesenchymal transition	[46], [47], [48]
12p13.33	*FOXM1 (3818)*	(GO:0046578) regulation of Ras protein signal transduction	[41]
19p13.2	*ELAVL1 (3312)*	(GO:0016441) post-transcriptional gene silencing	[49]
20q13.13	*SNAI1 (11128)*	(GO:0007498) mesoderm development, (GO:0061314) Notch signalling involved in heart development, (GO:0001837) epithelial to mesenchymal transition	[50]
21q22.2	*ERG (3446)*	(GO:0030154) cell differentiation	[40]
22q12.3	*RBFOX2 (9906)*	(GO:0000381) regulation of alternative mRNA splicing, via spliceosome	[51]

3. Discussion

In brain microvessels, direct arteriolar-to-venous shunt occurs in a pathological condition known as bAVM. Due to the complexity of events involved in early brain angiogenesis, a unique disease pathogenic model still lacks. Several studies aimed to characterize the mutational profile of bAVM tissues revealing the existence of *KRAS* and *BRAF* activating mutations [12,58]. By sequencing analysis, we identified 2 somatic mutations in the *KRAS* gene. Although their functional consequences are still uncharacterized, these data confirm

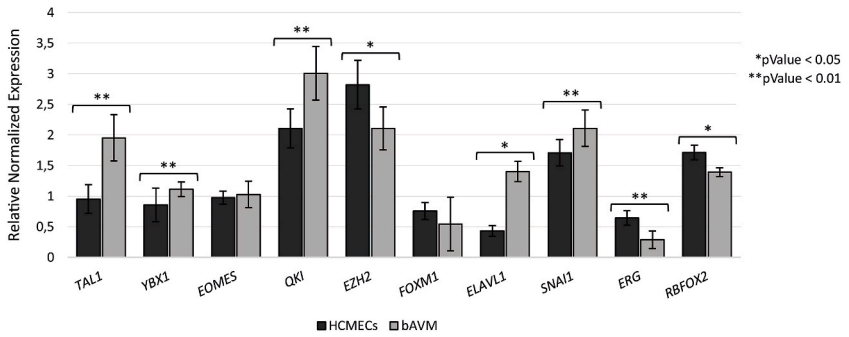

Fig. 6. qRT-PCR results. Quantitative realtime-PCR confirmed significative different gene expression between bAVM and HCMECs for all considered genes, with the exception of *EOMES* and *FOXM1*. Data are reported as relative expression value, normalized against the *ACTB* expression. Results are reported as the mean of three replicas, performed for each sample considered. Bonferroni-adjusted pValue.

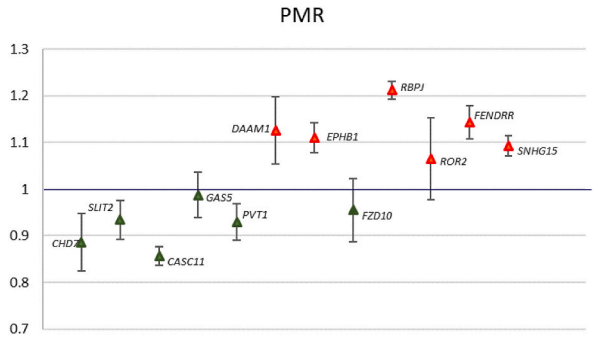

Fig. 7. Percent methylated reference results. For each validated gene, PMR is reported as the mean values of three replicas performed on 11 bAVM samples and compared against HCMECs. The blue line indicates the threshold to discriminate hypomethylated (green, PMR <1) and hypermethylated (red, PMR >1) genes in bAVM specimens. Bonferroni-adjusted pValue.

Table 4
Prioritized loci undergone aberrant CHG methylation events. The five listed genes were prioritized. For each, the chromosomal locus, the name and the HGNC Id, the biological function, the expression pattern in embryo and adults are described. HGNC: Human Genome Nomenclature Committee; EC: endothelial cells; HUVEC: human umbilical vascular endothelial cells; VSMC: vascular smooth muscle cells.

Locus	Gene (HGNC Id)	Biological activity	Expression in embryo	Expression in adult
1q21.3	*CERS2 (14076)*	Ceramide synthesis, oxidative stress response [52]	Placenta	Brain, artery ECs, liver, kidney
6q14.3	*TBX18 (11595)*	Heart, VSMC and vessel embryo development [53]	Brain, kidney, artery, heart,	Artery
9q33.3	*GAPVD1 (23375)*	Vesicle-mediated transport [54]	Placenta, brain,	HUVEC, VSMC
10p11.22	*NRP1 (8004)*	VEGF/semaphoring receptor, brain vasculature development [55]	Placenta, umbilical artery,	Brain, artery, retina
20q13.2	*SALL4 (15924)*	Neuron, heart, brain, anorectal development [56], [57]	Neural tube, heart,	Heart

the occurrence of KRAS mutations limited to bAVM ECs, However, further signals contribute to bAVM onset. During embryo development, several pathways control blood vessel formation and specialization. Among these, VEGF, Notch, Shh and TGF-β signalling perturbation can trigger the bAVM phenotype [10,11,17,59,60]. In order to obtain a wider landscape of bAVM tissue, we performed methylome analysis on ECs isolated from a bAVM specimen. Data were validated in further 10 samples. As expected, differential methylation events occur in genes encoding for proteins controlling vessel homeostasis. In addition, we found several differentially methylated noncoding genes. As described, they target transcription factors that regulate expression of genes involved in EC/VSMC cross-talk, suggesting that defective EC arterialization can result from impaired cell communication. According to current knowledge, . we observed *RBPJ* hypermethylation suggesting its down-expression. Selhorst et al. recently reported as endothelial *RBPJ* depletion contributes to bAVM vascular endothelium expansion [61]. Moreover, our data allowed to identify the two hedgehog coreceptors coding genes *GAS1* and *CDON*, hypermethylated in bAVM ECs and their role in endothelial integrity maintenance was recently shown [62]. However, the most accreditable hypothesis explaining sporadic bAVM onset is the aberrant expression of vessel differentiation markers during late angiogenesis. Most likely, impaired balance of ephrin B2 and EphB4 expression seems to trigger the arteriovenous

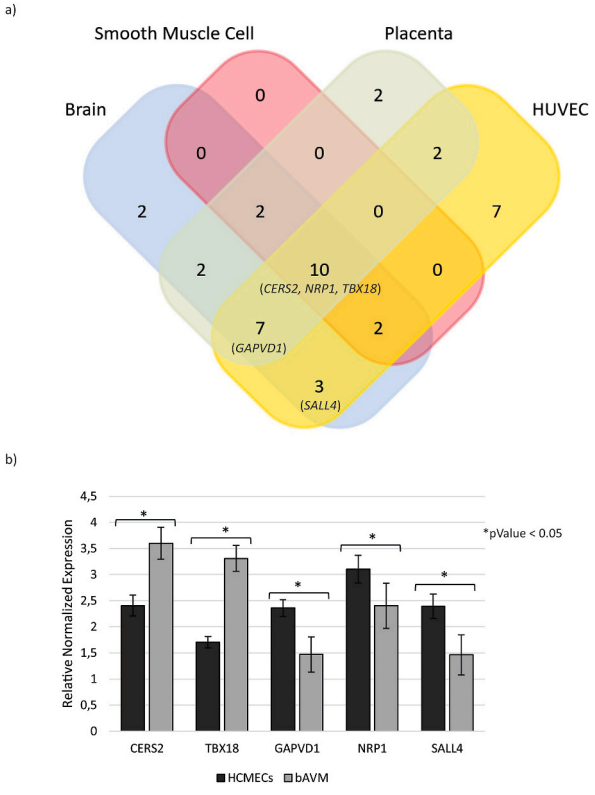

Fig. 8. CHG methylation. a) All 43 loci were clustered according to their expression site. Genes expressed in both brain and VSMCs, during embryo development were considered and their expression was compared by qRT-PCR, in bAVM vs HCMECs(b). Results are reported as the mean of three replicas, performed for each sample considered. All considered loci showed significant difference. Bonferroni-adjusted pValue.

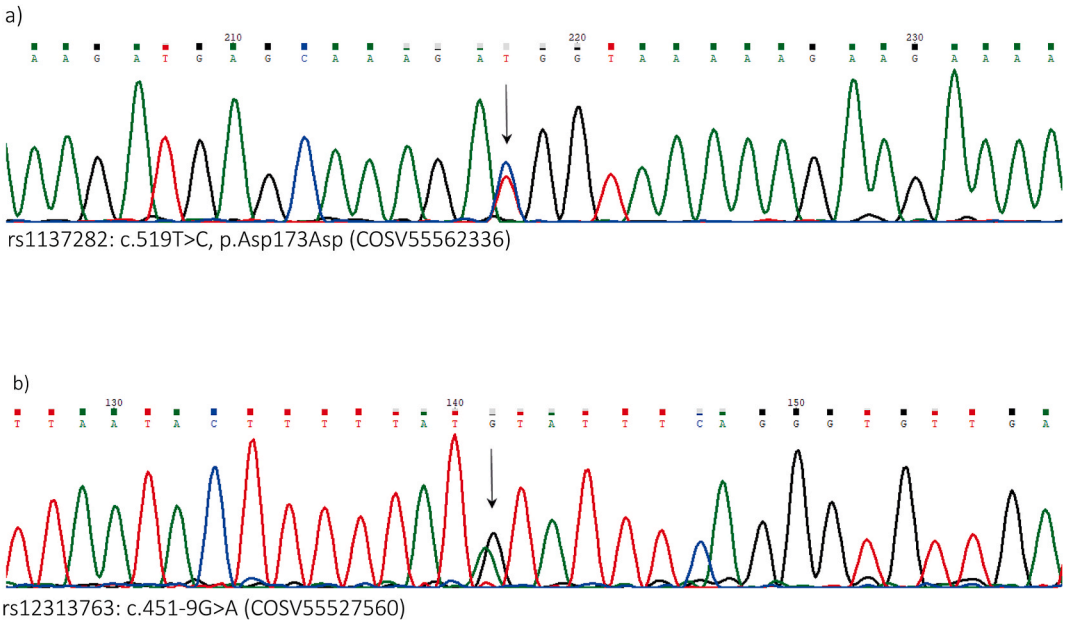

Fig. 9. *KRAS* somatic variants. a) Heterozygous synonymous variant rs1137282. b) Heterozygous intronic variant rs12313763. The arrows indicate the nucleotide substitutions.

phenotype [9]. In ECs, EphB4 binds RASA1 to negatively regulate the Ras-MAPK pathway [63]. Therefore, *RASA1* hypermethylation detected in our bAVM sample can result in failure of EphB4 regulation and, then, in venous EC identity loss.

3.1. EPHB1 expression and caveolae biogenesis in bAVM

In the context of the ephrin signalling, comparison of both *EFNB2* and *EPHB4* methylation profile between bAVM ECs and HCMECs showed no differences. However, we identified the hypermethylation of *EPHB1* gene. It encodes for a tyrosine kinase receptor expressed in brain ECs [64] and, in particular, in caveolae, where colocalizes with caveolin-1 (Cav-1). Increased Cav-1 ubiquitination results following *EPHB1* knock-out, leading to a reduced caveolae number in ECs [65]. In the central nervous system, caveolae predominantly abound in arteriolar ECs, where they lead cell polarization [66] and contribute to maintain BBB properties [67]. Finally, in EC caveolae, Cav-1 was also observed to colocalize with ALK1 and this interaction results in TGF-beta pathway modulation during angiogenesis [68,69]. We found *EPHB1* CpG islands hypermethylated in bAVM specimens, when compared to HCMECs, suggesting its down-expression. This can result in reduced caveolae number, decreased Cav-1 levels and, very likely, in perturbation of ALK-TGF-beta angiogenetic axis, suggesting that also *EPHB1*, together with *EPHB4* and *EFNB2*, can contribute to aberrant arterio-venous differentiation.

3.2. The role of ECM and EC/VSMC adhesion in bAVM

As above mentioned, correct vasculogenesis requires specific EC-ECM interactions. In this context, several differentially methylated genes in bAVM ECs were clustered in pathways related to the Wnt signalling. The *CHD7* gene is a Wnt downstream effector causes artery defects in CHARGE syndrome [70,71]. Although its role in small vessel development is not yet clear, it resulted hypomethylated in our bAVM ECs. We further confirmed the hypomethylation of both *FZD7* and *WNT7B*, known to be associated with vascular remodelling, stemness and EndMT when overexpressed [72], [73], and the hypermethylation of *FZD10* and *RYK*, both required for brain EC property maintenance [74–77]. Interestingly, several differentially methylated genes were clustered in the noncanonical planar cell polarity Wnt pathway, triggered by Wnt5a activation [78]. In detail, we observed hypermethylation of both *DAAM1* and *ROR2*. *WNT5A* mutations result in loss of arterial/venous differentiation during atrial septation [79]. This phenotype is rescued by Daam1. *DAAM1* was hypermethylated in our samples, suggesting its role in loss of EC identity. Ror2, instead, is an effector of both Wnt5a and Wnt7a. In detail, the Wnt5a/Ror2 axis was shown to induce VSMC proliferation [80] and EC polarity modulation by stabilizing adherens junctions [81,82]. Downstream of Wnt7a, Ror2 contributes to the correct vessel development, by promoting VEGFA signalling and perturbation of this cascade results in small vessel loss [83]. According to our data, *DAAM1* and *ROR2* hypermethylation could results in impaired EC polarity and, very likely, in reduced EC signals towards VSMCs. Taken together, these data suggest for the first time Wnt signature in bAVM lesions. In addition, we found differential methylation events occurring in several ECM genes involved in VSMC maturation and function. In particular, *COL4A1*, also known as vascular collagen, represents the major component of the vascular basement membrane and it was shown to contribute to arterial defects and VSMC loss [84,85]. It resulted hypomethylated in our sample further supporting that bAVM phenotype can be triggered by EC impaired expression of genes that control VSMC homeostasis.

3.3. Aberrant methylation in noncoding genes regulating neurovascular coupling

In the last few years, several noncoding RNAs were shown to regulate neurovascular development [86], . About lncRNA genes, here we focused on *GAS5*, *PVT1*, *SNHG15*, *CASC11*, *SOX2-OT* and *FENDRR*, according to transcripts they target and their confirmed expression in ECs. As above described, impaired methylation pattern was confirmed by qMSP on bisulfite-converted DNA sequencing. *CASC11* and *GAS5* overexpression was shown to trigger VSMC apoptosis [44,87]. In contrast, *GAS5* was shown to induce VSMC proliferation, when down-regulated [88,47]. However, role of these genes in EC/VSMC cross-talk requires further investigations. EC proliferation, instead, is reduced following *PVT1* overexpression [89]. Our methylation data suggest *CASC11*, *GAS5* and *PVT1* hypomethylation in bAVM ECs when compared to HCMECs, supporting the hypothesis that their dysregulation can contribute to the hyperproliferative phenotype of bAVM lesions. About hypermethylated lncRNA genes, *FENDRR* was shown to enhance artery EC pyroptosis, when down-expressed [90]. Finally, both *SOX2-OT* and *SNGH15* were recently related to VSMC and EC damage [91,92]. However, in order to clarify the mechanism by which these genes can contribute to bAVM development, we focused on their targets that include *TAL1*, *YBX1*, *EOMES*, *QKI*, *ELAVL1*, *SNAI1*, *EZH2*, *FOXM1*, *ERG* and *RBFOX2*. These encode for transcription factors that lead neurovascular development at embryo stage. In particular, they act by regulating biological processes including EndMT (*TAL1*, *SNAI1*) [37,38,93] and VSMC differentiation (*ELAVL1*, *QKI*) [35]. Both *TAL1* and *SNAI1* overexpression detected in bAVM suggests that these genes likely contribute to stemness in affected ECs. *EZH2* is a Polycomb-group family protein expressed in developing mouse endothelium and its inactivation impairs vascular wall due to increased ECM degradation [34] and it resulted down-expressed in our samples. Likewise, *QKI*, a RNA-binding protein controlling alternative splicing and mRNA export, is required for smooth muscle cell differentiation during embryonic blood vessel formation [32,94] and it resulted over-expressed in bAVM ECs. Moreover, about splicing regulation, down-expression of *ERG2* and *RBFOX2* was detected. *ERG2* is the endothelial-specific Early Growth Response (ERG) isoform expressed during embryo development [95]. Although little is known about its biological function in ECs, its splicing regulatory function related to RBFOX2 activity was demonstrated [36,40]. Taken together, these data suggest that EC identity loss in bAVM could be also triggered by defective neurovascular communication.

3.4. Possible role of the novel arteridin protein in bAVM pathogenesis

Finally, about lncRNA targeted transcripts, we focused on the *YBX1* gene, encoding for a double function protein. By binding the DNA, it acts on its repair. By binding the RNA, instead, it regulates pre-mRNA maturation and translation. *YBX1* is expressed in VSMCs where is targeted by GAS5 that inhibits its proteasome-mediated degradation [44]. Quantitative RT-PCR confirmed its overexpression in bAVM ECs, as well as the *GAS5* hypomethylation. In ECs, *YBX1* overexpression enhances the pro-angiogenetic phenotype [96]. Moreover, it binds the lncRNA PSR. The *PSR* gene, *P*henotype-*S*witching-*R*egulator, encodes for a novel characterized long noncoding RNA, recently described as abundant in VSMCs surrounding rat aorta. The transcript was identified in rat where, surprisingly, it was

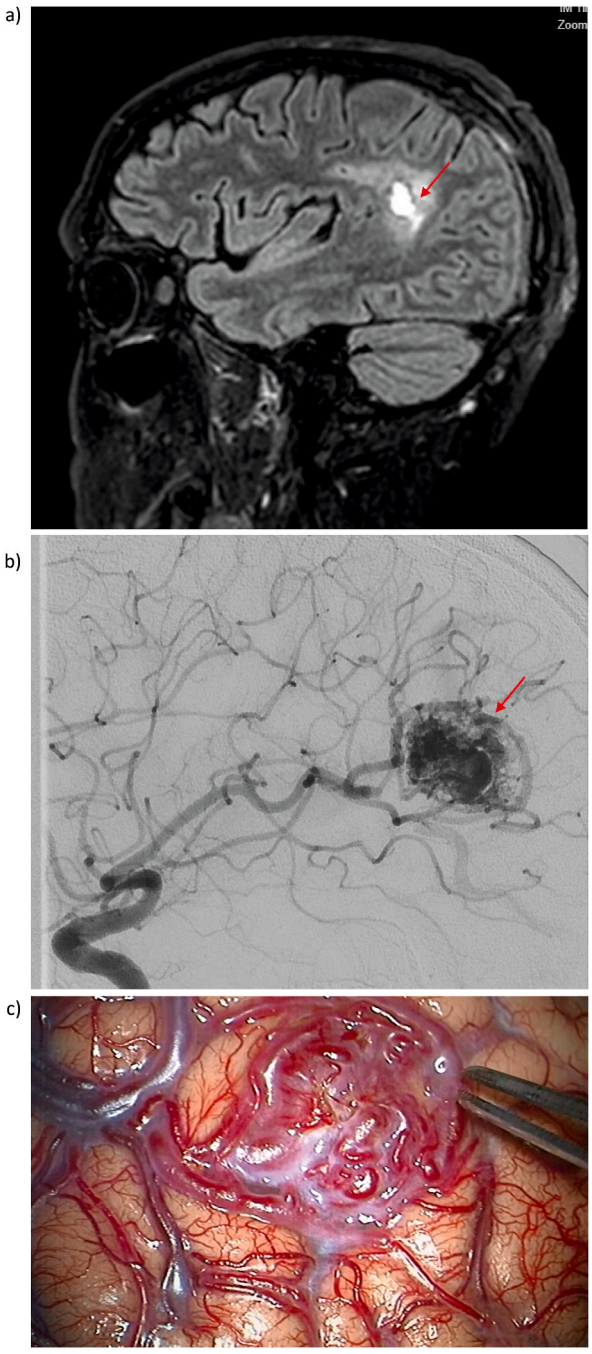

Fig. 10. Clinical features of bAVM lesion. a) MRI evidence of the lesion (indicated by the red arrow) in the right parietal area. b) Cerebral angiography for bAVM diagnosis confirmation. c) Microsurgical removal of the bAVM lesion.

also shown to encode for a novel protein, involved in endothelial phenotype switching during vascular remodelling and, therefore, called Arteridin [43]. Both lncPSR and Arteridin seem to bind YBX1, enhancing its nuclear translocation, where induces expression of target genes. Multiple alignment revealed that *PSR* is highly conserved in mammalian and, according to nucleotide sequence, its human ortholog seems to map to the *RASAL2-AS1* locus. Likewise, the arteridin human ortholog seems to map with the still uncharacterized 106 amino acid hCG1813082 protein (European Nucleotide Archive accession Id: EAW91016.1). Little is known about *RASAL2-AS1* function in mammalian cells however, according to these data, investigation of a possible RASAL2-AS1-arteridin/YBX1 axis in bAVM pathogenesis could highlight novel signalling impaired in aberrant vessel differentiation.

3.5. Aberrant CHG methylation of early angiogenesis related genes in bAVM

Cytosine methylation in CHG sequences mostly occurs during embryo development and its role in adults is still poor investigated [97]. Here, we identified several genes showing aberrant CHG methylation in bAVM ECs, when compared to HCMECs. According to their expression pattern, we focused on *CERS2*, *NRP1*, *TBX18*, *GAPVD1* and *SALL4* that were confirmed as dysregulated by qRT-PCR. Little is known about *GAPVD1* function [98]. *CERS2* and *TBX18* are involved in neuronal axon regeneration and epicardium development, respectively [89,99]. Therefore, the hypothesis of their possible role in bAVM pathogenesis is still elusive. The transcription factor *SALL4* is considered an embryonic stem cell marker and it resulted over-represented in venous malformation ECs [100]. In addition, it was recently shown to regulate proliferation, migration and sprouting during early angiogenesis [101]. Finally, the *NRP1* locus is essential for neurovascular development in zebrafish [102]. In brain ECs, it negatively regulates TGFβ-R2 activation, blocking endothelial sprouting. Perturbation of this signalling results in aberrant angiogenesis during early vessel development [55]. The pathway by which this mechanism occurs involves the same ALK1/Smad cascade, impaired in bAVM pathogenesis [103,104]. Further, NRP1 activity on angiogenesis is not only restricted to the ECs, but PDGF signalling modulation by NRP1 was also shown in VSMCs. Gain of function mutations in *NRP1*, as well as its increased expression, result in hyper-vascularized phenotypes and vessel dilatation [105]. Taken together, these findings encourage to strongly consider *NRP1* in bAVM pathogenesis.

3.6. Final remarks and limits of the study

Sporadic brain vascular phenotypes can result from aberrant gene expression occurring during embryo development and, together with somatic mutations, this is the most common mechanism considered for bAVM pathogenesis. By bisulfite-converted DNA sequencing performed on ECs isolated from bAVM specimen, we identified aberrant methylation pattern in both coding and noncoding genes, when compared to HCMECs. Enrichment analysis clustered these coding genes in pathways already linked to bAVM pathogenesis. In addition, vasculature remodelling triggered by ECM proteins was proposed as mechanism that contributes to vessel differentiation loss. Likewise, evidences of impaired crosstalk between ECs and VSMCs was discussed according to the differential methylation pattern observed in genes expressed in ECs but also regulating VSMC physiology.

Finally, together with conventional CpG methylation, we identified aberrant CHG methylation pattern in genes expressed at embryo stage. In adulthood, most of CHG methylation events occur in genes controlling brain and vasculature remodelling. Taken together, these findings encourage to consider impaired CHG methylation during early arterialization can contribute to bAVM progression. Reasons why aberrant CHG methylation occurs need to be clarified.

In this study, role of crosstalk between ECs and VSMCs has often been considered. However, the main limit of the study is the analysis performed only on ECs. In order to validate these data, further analyses on VSMCs are required. Moreover, *in-vivo* assays need to be performed to evaluate phenotypes triggered by loss/gain of functions in genes resulted differentially methylated in this study.

4. Materials and methods

4.1. Sample collection for methylome analysis

Methylome analysis was performed on ECs separated from a bAVM lesion. The donor was a 49-years old man. Diagnosis was performed by brain MRI, following episodes of loss of consciousness. The single lesion was identified in the right parietal area (nidus 2 × 2x2.5 cm, superficial venous drainage located, non-eloquent area) (Fig. 10a). Cerebral angiography confirmed a grade 1 Spetzler-Martin AVM, with an intra nidus aneurysm (Fig. 10b and c). The lesion was completely removed by the green-indocyanin guided microsurgical transnucal surgery. From biopsy, ECs were captured by using the MidiMacs/LSColumn/CD31^{+} system, previous collagenase/dispase enzymatic digestion [106]. The sample was treated with 0.1 % collagenase type IV/dispase (Gibco™, ThermoFisher Scientific, Carlsbad, CA, USA) in Hank's Balanced Salt Solution (Gibco™, ThermoFisher Scientific, Carlsbad, CA, USA) and Endothelial Cell Growth Medium MV (PromoCell) supplied with Supplement mix (PromoCell) and incubated at 37 °C for 4 h. Dissected cells were centrifuged at 300×*g* at 4 °C for 10 min and resuspended in the EC growth medium. From cell suspension, ECs were magnetically labelled with the CD31 MicroBead, human (©Miltenyi Biotec GmbH, Bergisch Gladbach, Germany) and separated on LS Columns (©Miltenyi Biotec GmbH, Bergisch Gladbach, Germany) by the MidiMACS™ Separator system (©Miltenyi Biotec GmbH, Bergisch Gladbach, Germany). Endothelial cells were collected in EC growth medium, phosphate buffered saline (PBS 1x) washed and directly used for both DNA and RNA purification. Culture maintenance was avoided to prevent cell loss due to the reduced cell number and the low viability rate of bAVM ECs.

4.2. Human cerebral microvascular endothelial cell (HCMECs) culture

In order to promote cell adhesion, second passage Human Cerebral Microvascular Endothelial Cells (HCMECs) (hCMEC/D3, Millipore) were cultured in Matrigel® Matrix (Corning, New York, NY, U.S.A.) coated T-25 flasks, with Endothelial Cell Growth Medium MV (PromoCell), supplied with Supplement mix (PromoCell) and 1 % of penicillin/streptomycin. Supplement mix comprises fetal calf serum (final concentration 0.02 ml/ml), endothelial cell growth supplement (final concentration 0.004 ml/ml), epidermal growth factor (final concentration 0.1 ng/ml), basic fibroblast growth factor (final concentration 1 ng/ml), heparin (final concentration 90 μg/ml), hydrocortisone (final concentration 1 μg/ml).Cultures were grown at 37 °C with 5 % CO_2. DNA purified from HCMECs was used for methylation profile comparison. RNA was purified and used as control for qRT-PCR assays.

4.3. DNA purification, bisulfite conversion and methylome sequencing

From 2×10^2 ECs, DNA was purified by the MagMAX™-96 DNA Multi-Sample Kit (Invitrogen™, ThermoFisher Scientific, Carlsbad, CA, USA), following manufacturer protocol and quantified by the Qubit fluorometer. Bisulfite conversion was performed by the Zymo Research EZ DNA Methylation-Gold Kit™ (Zymo Research Corporation). The Accel-NGS Methyl-Seq Library kit (Swift Biosciences, Inc.) was used to generate 150 paired-end libraries by using 100 ng of bisulfite-converted DNA as input, following datasheet instructions. Libraries were run on an Illumina NovaSeq6000.

4.4. Raw data quality control a bioinformatic analysis

Generated reads were quality checked by the FastQC software (Version 0.11.9) (https://www.bioinformatics.babraham.ac.uk/projects/fastqc/) and reads showing a Phred score >28 were selected for downstream analysis. Low quality reads and adapters were removed by the Trimmomatic tool (v.0.39) [107]. Selected bisulfite-converted reads were mapped against the GRCh38 Human Reference Genome by the BWA-meth algorithm [108]. Methylation biases and metrics were extracted by the MethylDackel software (https://github.com/dpryan79/MethylDackel). Differential methylation analysis was performed by the Metilene tool [109]. Output data were provided as differentially methylated both CpG and CHG regions.

4.5. Functional enrichment of differentially methylated genes

Differentially methylated genes were clustered according to the gene type as follow: Immunoglobulin Variable Region genes (IG_V_gene), Immunoglobulin Variable Region pseudogenes (IG_V_pseudogene), long noncoding RNAs (lncRNA), micro RNAs (miRNA), miscellaneous RNAs (misc_RNA), polymorphic pseudogenes, processed pseudogenes, protein coding genes, pseudogenes, ribozymes, rRNAs, rRNA pseudogenes, Ssmall Cajal body-specific RNAs (scaRNA), small nucleolar RNAs (snoRNA), small nuclear RNAs (snRNA), To be Experimentally Confirmed RNAs (TEC), constant chain T cell receptor genes (TR_C_gene), transcribed processed pseudogenes, transcribed unitary pseudogenes, transcribed unprocessed pseudogenes, unitary pseudogenes, unprocessed pseudogenes. Protein coding genes were clustered according to Reactome Pathway Database, by the FunRich tool [110]. For noncoding RNA enrichment analysis, the RNA interactome repository RNAInter v4.0 (http://www.rnainter.org/) was used [111]. Candidate genes undergoing differential methylation events in bAVM ECs and clustered in pathways controlling neurovascular development and blood-brain barrier integrity were prioritized and selected for validation.

4.6. Validation of CpG methylation by quantitative methylation specific PCR (qMSP)

Quantitative methylation specific PCR (qMSP) is a realtime-PCR based method useful to detect methylation level of a given chromosomal region. Among prioritized genes, methylation profile observed by the methylome sequencing was validated on the same sample and, to further confirm obtained data, in additional 10 samples belonging to subsequently recruited patients (SM6). Endothelial cell isolation and DNA purification were performed as previously described. Informed consent was obtained from all patients enrolled in the study.

Validated genes include *RPBJ*, *EPHB1*, *FZD10*, *DAAM1*, *ROR2*, *CHD7*, *SLIT2*, *CASC11*, *FENDRR*, *GAS5*, *PVT1*, *SNHG15*. Primers for differentially methylated CpG islands were designed according to the their nucleotide sequences reported in the UCSC Genome Browser (https://genome.ucsc.edu/index.html) [112], by the EpiDesigner tool (https://epidesigner.com/index.html) (SM7). Therefore, 500 ng genomic DNA isolated from bAVM ECs were bisulfite-treated by the EpiJET Bisulfite Conversion Kit (Thermo Fisher Scientific), following manufacturer protocol. Quantitative MSP was conducted as described: 50 ng bisulfite converted genomic DNA were added to 5 μl PowerUp™ SYBR™ Green Master Mix (2 ×) (PowerUp™ SYBR™ Green Master Mix, Applied Biosystems™, Thermo Fisher Scientific), 500 nM each primer and run on a QuantStudio 6 Real-time PCR system (Applied Biosystems, Foster, USA). Bisulfite-converted DNA purified from HCMECs was used as control to set up the standard curves for all considered genes. Results were normalized against the *ACTB*. For each reaction, three replicas were performed and results are reported as the mean value of all replicas, for all considered samples. Obtained data were expressed as Percent Methylated Reference (PMR), calculated as follow:

$$\mathrm{PMR}: \frac{\frac{CN\_MethTarget}{CN\_MethACTB}\ (bAVM\ sample)}{\frac{CN\_MethTarget}{CN\_MethACTB}\ (HCMECs)}$$

Where *CN_MethTarget* refers to the copy number of the methylated target gene and *CN_MethACTB* is the copy number of methylated *ACTB* gene.

Statistical analysis was performed by the Mann–Whitney *U* test. Significance was assessed for Bonferroni-adjusted pValue <0.05.

4.7. RNA purification and quantitative realtime-Polymerase Chain Reaction (qRT-PCR)

Quantitative realtime-Polymerase Chain Reaction (qRT-PCR) was performed to: i) confirm purity of ECs isolated from bAVM specimens; ii) evaluate expression of genes targeted by lncRNAs encoded by differentially methylated genes; iii) evaluate expression of genes underwent differential CHG methylation (SM7). RNA was purified by 1.5×10^3 ECs isolated from bAVM specimens and control HCMECs by the TRIzol™ RNA Isolation Reagent (Invitrogen, ThermoFisher Scientific, Waltham, MA, USA), according to manufacturer instruction and quantified by the NanoDrop. For quantitative analysis, 2 μg of total RNA were retrotranscribed by the SuperScript™ IV VILO™ Master Mix (SuperScript IV VILO Master Mix with ezDNase, Invitrogen®, Thermo Fisher Scientific). For gene expression evaluation, 5 ng of cDNA were amplified supplied with 200 nM of each specific primer and 5 μl PowerUp™ SYBR™ Green Master Mix ($2 \times$) (PowerUp™ SYBR™ Green Master Mix, Applied Biosystems™, Thermo Fisher Scientific). Amplification was performed on QuantStudio 6 Real-time PCR system (Applied Biosystems, Foster, USA). Relative expression levels were calculated by the $2^{-\Delta Ct}$ method normalized against the *ACTB* expression level. The expression analysis was performed on all 11 samples. For each sample, 3 replicas were performed. Results are reported as the mean of three replicas, for all included samples. The Kruskal-Wallis test was applied to assess the statistical significance of the observed fold changes. Obtained p-values were adjusted by the Bonferroni correction.

4.8. KRAS coding region sequencing

According to literature data, *KRAS* gain of function mutations occur in bAVM tissues. *KRAS* coding regions were sequenced in all considered bAVM specimens. Briefly, coding exons and intron-exon boundaries were amplified by the HotStarTaq Plus DNA Polymerase (Qiagen), by using 30 ng genomic DNA and 0.3 μM each primer, following manufacturer protocol. Primer pairs were designed according to the nucleotide sequence reported in the Ensembl repository (*KRAS*, Ensemble gene ID: ENSG00000133703) (SM7). Amplicons for DNA sequencing were obtained by the BigDye Terminator chemistry (BigDye™ Terminator v3.1 Cycle Sequencing Kit, Applied Biosystems®, Thermofisher Scientific) and run on a 3500 Genetic Analyzer (Applied Biosystems®, Thermofisher Scientific). Obtained sequences were aligned against the GRCh38 Genome assembly reference genome.

Statistical analysis

Statistical analysis was performed by the IBM SPSS 26.0 software (https://www.ibm.com/analytics/us/en/technology/spss/). Significance of both MS-PCR and qRT-PCR data was assessed by the non-parametric Kruskal-Wallis test for independent samples, due to both reduced sample size and not normal data distribution. Obtained p-values were adjusted by the Bonferroni correction. For each condition, 3 replicas were considered and results are reported as the mean of the three replicas for each sample.

CRediT authorship contribution statement

Concetta Scimone: Conceptualization, Writing – original draft. **Luigi Donato:** Data curation. **Simona Alibrandi:** Investigation. **Alfredo Conti:** Resources. **Carlo Bortolotti:** Resources. **Antonino Germanò:** Investigation. **Concetta Alafaci:** Resources. **Sergio Lucio Vinci:** Funding acquisition. **Rosalia D'Angelo:** Data curation, Writing – review & editing. **Antonina Sidoti:** Supervision, Validation.

Declaration of competing interest

The authors declare that they have no known competing financial interests or personal relationships that could have appeared to influence the work reported in this paper.

Appendix A. Supplementary data

Supplementary data to this article can be found online at https://doi.org/10.1016/j.heliyon.2024.e35126.

References

[1] J.A. Cain, B. Montibus, R.J. Oakey, Intragenic CpG islands and their impact on gene regulation, Front. Cell Dev. Biol. 10 (2022) 832348, https://doi.org/10.3389/fcell.2022.832348.

[2] B.F. Vanyushin, V.V. Ashapkin, DNA methylation in higher plants: past, present and future, Biochim. Biophys. Acta 1809 (2011) 360–368, https://doi.org/10.1016/j.bbagrm.2011.04.006.

[3] R. Lister, M. Pelizzola, R.H. Dowen, R.D. Hawkins, G. Hon, J. Tonti-Filippini, J.R. Nery, L. Lee, Z. Ye, Q.M. Ngo, et al., Human DNA methylomes at base resolution show widespread epigenomic differences, Nature 462 (2009) 315–322, https://doi.org/10.1038/nature08514.

[4] R. Lister, E.A. Mukamel, J.R. Nery, M. Urich, C.A. Puddifoot, N.D. Johnson, J. Lucero, Y. Huang, A.J. Dwork, M.D. Schultz, et al., Global epigenomic reconfiguration during mammalian brain development, Science 341 (2013) 1237905, https://doi.org/10.1126/science.1237905.

[5] K.E. Varley, J. Gertz, K.M. Bowling, S.L. Parker, T.E. Reddy, F. Pauli-Behn, M.K. Cross, B.A. Williams, J.A. Stamatoyannopoulos, G.E. Crawford, et al., Dynamic DNA methylation across diverse human cell lines and tissues, Genome Res. 23 (2013) 555–567, https://doi.org/10.1101/gr.147942.112.

[6] D. Goyal, R. Goyal, Angiogenic transformation in human brain micro endothelial cells: whole genome DNA methylation and transcriptomic analysis, Front. Physiol. 10 (2019) 1502, https://doi.org/10.3389/fphys.2019.01502.

[7] C.J. Chen, D. Ding, C.P. Derdeyn, G. Lanzino, R.M. Friedlander, A.M. Southerland, M.T. Lawton, J.P. Sheehan, Brain arteriovenous malformations: a review of natural history, pathobiology, and interventions, Neurology 95 (2020) 917–927, https://doi.org/10.1212/WNL.0000000000010968.

[8] H.U. Wang, Z.F. Chen, D.J. Anderson, Molecular distinction and angiogenic interaction between embryonic arteries and veins revealed by ephrin-B2 and its receptor Eph-B4, Cell 93 (1998) 741–753, https://doi.org/10.1016/s0092-8674(00)81436-1.

[9] K.K. Murai, E.B. Pasquale, Eph'ective signaling: forward, reverse and crosstalk, J. Cell Sci. 116 (2003) 2823–2832, https://doi.org/10.1242/jcs.00625.

[10] C. Yang, Y. Guo, C.C. Jadlowiec, X. Li, W. Lv, L.S. Model, M.J. Collins, Y. Kondo, A. Muto, C. Shu, et al., Vascular endothelial growth factor-A inhibits EphB4 and stimulates delta-like ligand 4 expression in adult endothelial cells, J. Surg. Res. 183 (2013) 478–486, https://doi.org/10.1016/j.jss.2013.01.009.

[11] I. Giarretta, C.L. Sturiale, I. Gatto, S. Pacioni, E. Gaetani, A. Porfidia, A. Puca, I. Palucci, P. Tondi, A. Olivi, et al., Sonic hedgehog is expressed in human brain arteriovenous malformations and induces arteriovenous malformations in vivo, J. Cerebr. Blood Flow Metabol. 41 (2021) 324–335, https://doi.org/10.1177/0271678X20912405.

[12] S.I. Nikolaev, S. Vetiska, X. Bonilla, E. Boudreau, S. Jauhiainen, B. Rezai Jahromi, N. Khyzha, P.V. DiStefano, S. Suutarinen, T.R. Kiehl, et al., Somatic activating KRAS mutations in arteriovenous malformations of the brain, N. Engl. J. Med. 378 (2018) 250–261, https://doi.org/10.1056/NEJMoa1709449.

[13] M. Corada, F. Orsenigo, M.F. Morini, M.E. Pitulescu, G. Bhat, D. Nyqvist, F. Breviario, V. Conti, A. Briot, M.L. Iruela-Arispe, et al., Sox17 is indispensable for acquisition and maintenance of arterial identity, Nat. Commun. 4 (2013) 2609, https://doi.org/10.1038/ncomms3609.

[14] H.S. Jung, G. Uenishi, M.A. Park, P. Liu, K. Suknuntha, M. Raymond, Y.J. Choi, J.A. Thomson, I.M. Ong, I.I. Slukvin, SOX17 integrates HOXA and arterial programs in hemogenic endothelium to drive definitive lympho-myeloid hematopoiesis, Cell Rep. 34 (2021) 108758, https://doi.org/10.1016/j.celrep.2021.108758.

[15] H. Pendeville, M. Winandy, I. Manfroid, O. Nivelles, P. Motte, V. Pasque, B. Peers, I. Struman, J.A. Martial, M.L. Voz, Zebrafish Sox7 and Sox18 function together to control arterial-venous identity, Dev. Biol. 317 (2008) 405–416, https://doi.org/10.1016/j.ydbio.2008.01.028.

[16] D. Zhang, X. Qiao, L. Wang, L. Zhang, J. Yao, X. Wu, T. Yu, K.I. Boström, Y. Yao, Skip is essential for Notch signaling to induce Sox2 in cerebral arteriovenous malformations, Cell. Signal. 68 (2020) 109537, https://doi.org/10.1016/j.cellsig.2020.109537.

[17] C.M. Nielsen, X. Zhang, K. Raygor, S. Wang, A.W. Bollen, R.A. Wang, Endothelial Rbpj deletion normalizes Notch4-induced brain arteriovenous malformation in mice, J. Exp. Med. 220 (2023) e20211390, https://doi.org/10.1084/jem.20211390.

[18] X. Qiao, D. Zhang, L. Zhang, J. Yao, X. Wu, X. Cai, K.I. Boström, Y. Yao, Pronethalol decreases RBPJκ to reduce Sox2 in cerebral arteriovenous malformation, Vasc. Med. 25 (2020) 569–571, https://doi.org/10.1177/1358863X20942833.

[19] E. Coccia, L. Valeri, R. Zuntini, S.G. Caraffi, F. Peluso, L. Pagliai, A. Vezzani, Z. Pietrangiolillo, F. Leo, N. Melli, et al., Prenatal clinical findings in RASA1-related capillary malformation-arteriovenous malformation syndrome, Genes 14 (2023) 549, https://doi.org/10.3390/genes14030549.

[20] J. Greysson-Wong, R. Rode, J.R. Ryu, J.L. Chan, P. Davari, K.D. Rinker, S.J. Childs, Rasa1-related arteriovenous malformation is driven by aberrant venous signalling, Development 150 (2023) dev201820, https://doi.org/10.1242/dev.201820.

[21] W. Du, L. Huang, X. Tang, J. Li, X. Li, Ephrin-A5 is involved in retinal neovascularization in a mouse model of oxygen-induced retinopathy, BioMed Res. Int. 2020 (2020) 7161027, https://doi.org/10.1155/2020/7161027.

[22] G.Z. Chen, Y. Ke, K. Qin, M.Q. Dong, S.J. Zeng, X.F. Lin, S.Q. Zhan, K. Tang, C. Peng, X.W. Ding, et al., Analysis of the expression of angioarchitecture-related factors in patients with cerebral arteriovenous malformation, Chin. Med. J. (Engl). 130 (2017) 2465–2472, https://doi.org/10.4103/0366-6999.216413.

[23] C.M. Nielsen, H. Cuervo, V.W. Ding, Y. Kong, E.J. Huang, R.A. Wang, Deletion of Rbpj from postnatal endothelium leads to abnormal arteriovenous shunting in mice, Development 141 (2014) 3782–3792, https://doi.org/10.1242/dev.108951.

[24] X. Niu, X. Li, Z. Feng, Q. Han, J. Li, Y. Liu, K. Zhang, EDIL3 and VEGF synergistically affect angiogenesis in endothelial cells, Clin. Cosmet. Invest. Dermatol. 16 (2023) 1269–1277, https://doi.org/10.2147/CCID.S411253.

[25] L.F. Yousif, J. Di Russo, L. Sorokin, Laminin isoforms in endothelial and perivascular basement membranes, Cell Adhes. Migrat. 7 (2013) 101–110, https://doi.org/10.4161/cam.22680.

[26] S. Gao, J. Nelson, S. Weinsheimer, E.A. Winkler, C. Rutledge, A.A. Abla, N. Gupta, J.T. Shieh, D.L. Cooke, S.W. Hetts, et al., Somatic mosaicism in the MAPK pathway in sporadic brain arteriovenous malformation and association with phenotype, J. Neurosurg. 136 (2021) 148–155, https://doi.org/10.3171/2020.11.JNS202031.

[27] H. Xu, R. Huo, H. Li, Y. Jiao, J. Weng, J. Wang, Z. Yan, J. Zhang, S. Zhao, Q. He, et al., KRAS mutation-induced EndMT of brain arteriovenous malformation is mediated through the TGF-β/BMP-SMAD4 pathway. Stroke Vasc, Neurol. 8 (2023) 197–206, https://doi.org/10.1136/svn-2022-001700.

[28] G.E. Davis, D.R. Senger, Endothelial extracellular matrix: biosynthesis, remodeling, and functions during vascular morphogenesis and neovessel stabilization, Circ. Res. 97 (2005) 1093–1107, https://doi.org/10.1161/01.RES.0000191547.64391.e3.

[29] T. Wei, G.T. Richter, H. Zhang, R.W. Sun, C.H. Smith, G.M. Strub, Extracranial arteriovenous malformations demonstrate dysregulated TGF-β/BMP signaling and increased circulating TGF-β1, Sci. Rep. 12 (2022) 16612, https://doi.org/10.1038/s41598-022-21217-0.

[30] G.J. Li, Y. Yang, G.K. Yang, J. Wan, D.L. Cui, Z.H. Ma, L.J. Du, G.M. Zhang, Slit2 suppresses endothelial cell proliferation and migration by inhibiting the VEGF-Notch signaling pathway, Mol. Med. Rep. 15 (2017) 1981–1988, https://doi.org/10.3892/mmr.2017.6240.

[31] X. Ding, Q. An, W. Zhao, Y. Song, X. Tang, J. Wang, C.C. Chang, G. Zhao, T. Hsiai, G. Fan, et al., Distinct patterns of responses in endothelial cells and smooth muscle cells following vascular injury, JCI Insight 7 (2022) e153769, https://doi.org/10.1172/jci.insight.153769.

[32] Z. Li, N. Takakura, Y. Oike, T. Imanaka, K. Araki, T. Suda, T. Kaname, T. Kondo, K. Abe, K. Yamamura, Defective smooth muscle development in qkI-deficient mice, Dev. Growth Differ. 45 (2003) 449–462, https://doi.org/10.1111/j.1440-169x.2003.00712.x.

[33] N.L. Boyd, S.K. Dhara, R. Rekaya, E.A. Godbey, K. Hasneen, R.R. Rao, F.D.3rd West, B.A. Gerwe, S.L. Stice, BMP4 promotes formation of primitive vascular networks in human embryonic stem cell-derived embryoid bodies, Exp. Biol. Med. (Maywood). 232 (2007) 833–843.

[34] P. Delgado-Olguín, L.T. Dang, D. He, S. Thomas, L. Chi, T. Sukonnik, N. Khyzha, M.W. Dobenecker, J.E. Fish, B.G. Bruneau, Ezh2-mediated repression of a transcriptional pathway upstream of Mmp9 maintains integrity of the developing vasculature, Development 141 (2014) 4610–4617, https://doi.org/10.1242/dev.112607.

[35] A. Régent, K.H. Ly, S. Lofek, G. Clary, M. Tamby, N. Tamas, C. Federici, C. Broussard, P. Chafey, E. Liaudet-Coopman, et al., Proteomic analysis of vascular smooth muscle cells in physiological condition and in pulmonary arterial hypertension: toward contractile versus synthetic phenotypes, Proteomics 16 (2016) 2637–2649, https://doi.org/10.1002/pmic.201500006.

[36] P.A. Murphy, V.L. Butty, P.L. Boutz, S. Begum, A.L. Kimble, P.A. Sharp, C.B. Burge, R.O. Hynes, Alternative RNA splicing in the endothelium mediated in part by Rbfox2 regulates the arterial response to low flow, Elife 7 (2018) e29494, https://doi.org/10.7554/eLife.29494.

[37] K. Chandran Latha, A. Sreekumar, V. Beena, B.S.S. Raj, R.B. Lakkappa, R. Kalyani, R. Nair, S.R. Kalpana, C.C. Kartha, S. Surendran, Shear stress alterations activate BMP4/pSMAD5 signaling and induce endothelial mesenchymal transition in varicose veins, Cells 10 (2021) 3563, https://doi.org/10.3390/cells10123563.

[38] C. Collart, A. Ciccarelli, K. Ivanovitch, I. Rosewell, S. Kumar, G. Kelly, A. Edwards, J.C. Smith, The migratory pathways of the cells that form the endocardium, dorsal aortae, and head vasculature in the mouse embryo, BMC Dev. Biol. 21 (2021) 8, https://doi.org/10.1186/s12861-021-00239-3.

[39] L.T.G. Harland, C.S. Simon, A.D. Senft, I. Costello, L. Greder, I. Imaz-Rosshandler, B. Göttgens, J.C. Marioni, E.K. Bikoff, C. Porcher, et al., The T-box transcription factor Eomesodermin governs haemogenic competence of yolk sac mesodermal progenitors, Nat. Cell Biol. 23 (2021) 61–74, https://doi.org/10.1038/s41556-020-00611-8.

[40] V. Markova, L. Bogdanov, E. Velikanova, A. Kanonykina, A. Frolov, D. Shishkova, A. Lazebnaya, A. Kutikhin, Endothelial cell markers are inferior to vascular smooth muscle cells markers in staining vasa vasorum and are non-specific for distinct endothelial cell lineages in clinical samples, Int. J. Mol. Sci. 24 (2023) 1959, https://doi.org/10.3390/ijms24031959.

[41] T. Wu, N. Li, Q. Zhang, R. Liu, H. Zhao, Z. Fan, L. Zhuo, Y. Yang, Y. Xu, MKL1 fuels ROS-induced proliferation of vascular smooth muscle cells by modulating FOXM1 transcription, Redox Biol. 59 (2023) 102586, https://doi.org/10.1016/j.redox.2022.102586.

[42] K.J. Carroll, V. Esain, M.K. Garnaas, M. Cortes, M.C. Dovey, S. Nissim, G.M. Frechette, S.Y. Liu, W. Kwan, C.C. Cutting, et al., Estrogen defines the dorsal-ventral limit of VEGF regulation to specify the location of the hemogenic endothelial niche, Dev. Cell 29 (2014) 437–453, https://doi.org/10.1016/j.devcel.2014.04.012.

[43] J. Yu, W. Wang, J. Yang, Y. Zhang, X. Gong, H. Luo, N. Cao, Z. Xu, M. Tian, P. Yang, et al., LncRNA PSR regulates vascular remodeling through encoding a novel protein arteridin, Circ. Res. 131 (2022) 768–787, https://doi.org/10.1161/CIRCRESAHA.122.321080. Erratum in: Circ. Res. 2023, 133, e17.

[44] X. He, S. Wang, M. Li, L. Zhong, H. Zheng, Y. Sun, Y. Lai, X. Chen, G. Wei, X. Si, et al., Long noncoding RNA GAS5 induces abdominal aortic aneurysm formation by promoting smooth muscle apoptosis, Theranostics 9 (2019) 5558–5576, https://doi.org/10.7150/thno.34463.

[45] E.P. van der Veer, R.G. de Bruin, A.O. Kraaijeveld, M.R. de Vries, I. Bot, T. Pera, F.M. Segers, S. Trompet, J.M. van Gils, M.K. Roeten, et al., Quaking, an RNA-binding protein, is a critical regulator of vascular smooth muscle cell phenotype, Circ. Res. 113 (2013) 1065–1075, https://doi.org/10.1161/CIRCRESAHA.113.301302.

[46] H.Y. Zhong, C. Yuan, X.L. Liu, Q.Q. Wang, X. Li, Y.C. Zhao, X. Li, D.D. Liu, T.F. Zheng, M. Zhang, Mechanical stretch aggravates vascular smooth muscle cell apoptosis and vascular remodeling by downregulating EZH2, Int. J. Biochem. Cell Biol. 151 (2022) 106278, https://doi.org/10.1016/j.biocel.2022.106278.

[47] T. Le, X. He, J. Huang, S. Liu, Y. Bai, K. Wu, Knockdown of long noncoding RNA GAS5 reduces vascular smooth muscle cell apoptosis by inactivating EZH2-mediated RIG-I signaling pathway in abdominal aortic aneurysm, J. Transl. Med. 19 (2021) 466, https://doi.org/10.1186/s12967-021-03023-w.

[48] R.A. Soto, M.A.T. Najia, M. Hachimi, J.M. Frame, G.A. Yette, E. Lummertz da Rocha, K. Stankunas, G.Q. Daley, T.E. North, Sequential regulation of hemogenic fate and hematopoietic stem and progenitor cell formation from arterial endothelium by Ezh1/2, Stem Cell Rep. 16 (2021) 1718–1734, https://doi.org/10.1016/j.stemcr.2021.05.014.

[49] L. Gao, J. Yang, Y. Li, K. Liu, H. Sun, J. Tang, Z. Xia, L. Zhang, Z. Hu, Long noncoding RNA SCIRT promotes HUVEC angiogenesis via stabilizing VEGFA mRNA induced by hypoxia, Oxid. Med. Cell. Longev. 2022 (2022) 9102978, https://doi.org/10.1155/2022/9102978.

[50] C.L. Karthika, V. Venugopal, B.J. Sreelakshmi, S. Krithika, J.M. Thomas, M. Abraham, C.C. Kartha, A. Rajavelu, S. Sumi, Oscillatory shear stress modulates Notch-mediated endothelial mesenchymal plasticity in cerebral arteriovenous malformations, Cell. Mol. Biol. Lett. 28 (2023) 22, https://doi.org/10.1186/s11658-023-00436-x.

[51] L. Liu, D. Kryvokhyzha, C. Rippe, A. Jacob, A. Borreguero-Muñoz, K.G. Stenkula, O. Hansson, C.W.J. Smith, S.A. Fisher, K. Swärd, Myocardin regulates exon usage in smooth muscle cells through induction of splicing regulatory factors, Cell. Mol. Life Sci. 79 (2022) 459, https://doi.org/10.1007/s00018-022-04497-7.

[52] S. Choi, J.A. Kim, H.Y. Li, K.O. Shin, G.T. Oh, Y.M. Lee, S. Oh, Y. Pewzner-Jung, A.H. Futerman, S.H. Suh, KCa 3.1 upregulation preserves endothelium-dependent vasorelaxation during aging and oxidative stress, Aging Cell 15 (2016) 801–810, https://doi.org/10.1111/acel.12502.

[53] N. Ikeda, N. Nakazawa, Y. Kurata, H. Yaura, F. Taufiq, H. Minato, A. Yoshida, H. Ninomiya, Y. Nakayama, M. Kuwabara, et al., Tbx18-positive cells differentiated from murine ES cells serve as proepicardial progenitors to give rise to vascular smooth muscle cells and fibroblasts, Biomed. Res. 38 (2017) 229–238, https://doi.org/10.2220/biomedres.38.229.

[54] H. Kim, H. Oh, Y.S. Oh, J. Bae, N.H. Hong, S.J. Park, S. Ahn, M. Lee, S. Rhee, S.H. Lee, et al., SPIN90, an adaptor protein, alters the proximity between Rab5 and Gapex5 and facilitates Rab5 activation during EGF endocytosis, Exp. Mol. Med. 51 (2019) 1–14, https://doi.org/10.1038/s12276-019-0284-5.

[55] S. Hirota, T.P. Clements, L.K. Tang, J.E. Morales, H.S. Lee, S.P. Oh, G.M. Rivera, D.S. Wagner, J.H. McCarty, Neuropilin 1 balances β8 integrin-activated TGFβ signaling to control sprouting angiogenesis in the brain, Development 142 (2015) 4363–4373, https://doi.org/10.1242/dev.113746.

[56] P. Ghosh, J.M. Maurer, C.G. Sagerström, Analysis of novel caudal hindbrain genes reveals different regulatory logic for gene expression in rhombomere 4 versus 5/6 in embryonic zebrafish, Neural Dev. 13 (2018) 13, https://doi.org/10.1186/s13064-018-0112-y.

[57] M. Warren, W. Wang, S. Spiden, D. Chen-Murchie, D. Tannahill, K.P. Steel, A. Bradley, A Sall4 mutant mouse model useful for studying the role of Sall4 in early embryonic development and organogenesis, Genesis 45 (2007) 51–58, https://doi.org/10.1002/dvg.20264.

[58] O. Bameri, M. Salarzaei, F. Parooie, KRAS/BRAF mutations in brain arteriovenous malformations: a systematic review and meta-analysis, Intervent Neuroradiol. 27 (2021) 539–546, https://doi.org/10.1177/1591019920982810.

[59] C. Scimone, L. Donato, C. Alafaci, F. Granata, C. Rinaldi, M. Longo, R. D'Angelo, A. Sidoti, High-throughput sequencing to detect novel likely gene-disrupting variants in pathogenesis of sporadic brain arteriovenous malformations, Front. Genet. 11 (2020) 146, https://doi.org/10.3389/fgene.2020.00146.

[60] C. Scimone, F. Granata, M. Longo, E. Mormina, C. Turiaco, A.A. Caragliano, L. Donato, A. Sidoti, R. D'Angelo, Germline mutation enrichment in pathways controlling endothelial cell homeostasis in patients with brain arteriovenous malformation: implication for molecular diagnosis, Int. J. Mol. Sci. 21 (2020) 4321, https://doi.org/10.3390/ijms21124321.

[61] S. Selhorst, S. Nakisli, S. Kandalai, S. Adhicary, C.M. Nielsen, Pathological pericyte expansion and impaired endothelial cell-pericyte communication in endothelial Rbpj deficient brain arteriovenous malformation, Front. Hum. Neurosci. 16 (2022) 974033, https://doi.org/10.3389/fnhum.2022.974033.

[62] C. Chapouly, P.L. Hollier, S. Guimbal, L. Cornuault, A.P. Gadeau, M.A. Renault, Desert hedgehog-driven endothelium integrity is enhanced by Gas1 (growth arrest-specific 1) but negatively regulated by cdon (cell adhesion molecule-related/downregulated by oncogenes), Arterioscler. Thromb. Vasc. Biol. 40 (2020) e336–e349, https://doi.org/10.1161/ATVBAHA.120.314441.

[63] D. Chen, M.A. Van der Ent, N.L. Lartey, P.D. King, EPHB4-RASA1-Mediated negative regulation of ras-MAPK signaling in the vasculature: implications for the treatment of EPHB4- and RASA1-related vascular anomalies in humans, Pharmaceuticals 16 (2023) 165, https://doi.org/10.3390/ph16020165.

[64] R.H. Adams, G.A. Wilkinson, C. Weiss, F. Diella, N.W. Gale, U. Deutsch, W. Risau, R. Klein, Roles of ephrinB ligands and EphB receptors in cardiovascular development: demarcation of arterial/venous domains, vascular morphogenesis, and sprouting angiogenesis, Genes Dev. 13 (1999) 295–306, https://doi.org/10.1101/gad.13.3.295.

[65] C. Tiruppathi, S.C. Regmi, D.M. Wang, G.C.H. Mo, P.T. Toth, S.M. Vogel, R.V. Stan, M. Henkemeyer, R.D. Minshall, J. Rehman, et al., EphB1 interaction with caveolin-1 in endothelial cells modulates caveolae biogenesis, Mol. Biol. Cell 31 (2020) 1167–1182, https://doi.org/10.1091/mbc.E19-12-0713.

[66] P.R. Norden, Z. Sun, G.E. Davis, Control of endothelial tubulogenesis by Rab and Ral GTPases, and apical targeting of caveolin-1-labeled vacuoles, PLoS One 15 (2020) e0235116, https://doi.org/10.1371/journal.pone.0235116.

[67] B.W. Chow, V. Nuñez, L. Kaplan, A.J. Granger, K. Bistrong, H.L. Zucker, P. Kumar, B.L. Sabatini, C. Gu, Caveolae in CNS arterioles mediate neurovascular coupling, Nature 579 (2020) 106–110, https://doi.org/10.1038/s41586-020-2026-1.

[68] J.F. Santibanez, F.J. Blanco, E.M. Garrido-Martin, F. Sanz-Rodriguez, M.A. del Pozo, C. Bernabeu, Caveolin-1 interacts and cooperates with the transforming growth factor-beta type I receptor ALK1 in endothelial caveolae, Cardiovasc. Res. 77 (2008) 791–799, https://doi.org/10.1093/cvr/cvm097.

[69] R. Samarakoon, S.P. Higgins, C.E. Higgins, P.J. Higgins, The TGF-β1/p53/PAI-1 signaling Axis in vascular senescence: role of caveolin-1, Biomolecules 9 (2019) 341, https://doi.org/10.3390/biom9080341.

[70] V. Randall, K. McCue, C. Roberts, V. Kyriakopoulou, S. Beddow, A.N. Barrett, F. Vitelli, K. Prescott, C. Shaw-Smith, K. Devriendt, et al., Great vessel development requires biallelic expression of Chd7 and Tbx1 in pharyngeal ectoderm in mice, J. Clin. Invest. 119 (2009) 3301–3310, https://doi.org/10.1172/JCI37561.

[71] K. Fujita, R. Ogawa, S. Kawawaki, K. Ito, Roles of chromatin remodelers in maintenance mechanisms of multipotency of mouse trunk neural crest cells in the formation of neural crest-derived stem cells, Mech. Dev. 133 (2014) 126–145, https://doi.org/10.1016/j.mod.2014.05.001.

[72] Z. Zhang, Y. Xu, C. Zhao, Fzd7/Wnt7b signaling contributes to stemness and chemoresistance in pancreatic cancer, Cancer Med. 10 (2021) 3332–3345, https://doi.org/10.1002/cam4.3819.

[73] K. Yuan, M.E. Orcholski, C. Panaroni, E.M. Shuffle, N.F. Huang, X. Jiang, W. Tian, E.K. Vladar, L. Wang, M.R. Nicolls, et al., Activation of the Wnt/planar cell polarity pathway is required for pericyte recruitment during pulmonary angiogenesis, Am. J. Pathol. 185 (2015) 69–84, https://doi.org/10.1016/j.ajpath.2014.09.013.

[74] Z. Wang, W. Shu, M.M. Lu, E.E. Morrisey, Wnt7b activates canonical signaling in epithelial and vascular smooth muscle cells through interactions with Fzd1, Fzd10, and LRP5, Mol. Cell Biol. 25 (2005) 5022–5030, https://doi.org/10.1128/MCB.25.12.5022-5030.2005.

[75] K. Kumawat, M.H. Menzen, I.S. Bos, H.A. Baarsma, P. Borger, M. Roth, M. Tamm, A.J. Halayko, M. Simoons, A. Prins, et al., Noncanonical WNT-5A signaling regulates TGF-β-induced extracellular matrix production by airway smooth muscle cells, Faseb. J. 27 (2013) 1631–1643, https://doi.org/10.1096/fj.12-217539.

[76] B. Hot, J. Valnohova, E. Arthofer, K. Simon, J. Shin, M. Uhlén, E. Kostenis, J. Mulder, G. Schulte, FZD10-Gα13 signalling axis points to a role of FZD10 in CNS angiogenesis, Cell. Signal. 32 (2017) 93–103, https://doi.org/10.1016/j.cellsig.2017.01.023.

[77] T. Skaria, E. Bachli, G. Schoedon, Wnt5A/Ryk signaling critically affects barrier function in human vascular endothelial cells, Cell Adhes. Migrat. 11 (2017) 24–38, https://doi.org/10.1080/19336918.2016.1178449.

[78] S. Yanai, M. Wakayama, H. Nakayama, M. Shinozaki, H. Tsukuma, N. Tochigi, T. Nemoto, T. Saji, K. Shibuya, Implication of overexpression of dishevelled-associated activator of morphogenesis 1 (Daam-1) for the pathogenesis of human Idiopathic Pulmonary Arterial Hypertension (IPAH), Diagn. Pathol. 12 (2017) 25, https://doi.org/10.1186/s13000-017-0614-7.

[79] D. Li, A. Angermeier, J. Wang, Planar cell polarity signaling regulates polarized second heart field morphogenesis to promote both arterial and venous pole septation, Development 146 (2019) dev181719, https://doi.org/10.1242/dev.181719.

[80] Y. Shi, H. Li, J. Gu, Y. Gong, X. Xie, D. Liao, L. Qin, Wnt5a/Ror2 promotes vascular smooth muscle cells proliferation via activating PKC, Folia Histochem. Cytobiol. 60 (2022) 271–279, https://doi.org/10.5603/FHC.a2022.0026.

[81] J.R. Carvalho, I.C. Fortunato, C.G. Fonseca, A. Pezzarossa, P. Barbacena, M.A. Dominguez-Cejudo, F.F. Vasconcelos, N.C. Santos, F.A. Carvalho, C.A. Franco, Non-canonical Wnt signaling regulates junctional mechanocoupling during angiogenic collective cell migration, Elife 8 (2019) e45853, https://doi.org/10.7554/eLife.45853.

[82] P. Bougaran, M.L. Bats, V. Delobel, S. Rubin, J. Vaurs, T. Couffinhal, C. Duplàa, P. Dufourcq, ROR2/PCP a new pathway controlling endothelial cell polarity under flow conditions, Arterioscler. Thromb. Vasc. Biol. 43 (2023) 1199–1218, https://doi.org/10.1161/ATVBAHA.123.319106.

[83] A. Chakraborty, A. Nathan, M. Orcholski, S. Agarwal, E.A. Shamskhou, N. Auer, A. Mitra, E.S. Guardado, G. Swaminathan, D.F. Condon, et al., Wnt7a deficit is associated with dysfunctional angiogenesis in pulmonary arterial hypertension, Eur. Respir. J. 61 (2023) 2201625, https://doi.org/10.1183/13993003.01625-2022.

[84] J. Ratelade, N. Mezouar, V. Domenga-Denier, A. Rochey, E. Plaisier, A. Joutel, Severity of arterial defects in the retina correlates with the burden of intracerebral haemorrhage in COL4A1-related stroke, J. Pathol. 244 (2018) 408–420, https://doi.org/10.1002/path.5023.

[85] A.A. Kumar, N. Yeo, M. Whittaker, P. Attra, T.R. Barrick, L.R. Bridges, D.W. Dickson, M.M. Esiri, C.W. Farris, D. Graham, et al., Vascular collagen type-IV in hypertension and cerebral small vessel disease, Stroke 53 (2022) 3696–3705, https://doi.org/10.1161/STROKEAHA.122.037761.

[86] K.J. Yin, M. Hamblin, Y.E. Chen, Non-coding RNAs in cerebral endothelial pathophysiology: emerging roles in stroke, Neurochem. Int. 77 (2014) 9–16, https://doi.org/10.1016/j.neuint.2014.03.013.

[87] K. Tao, Z. Hu, Y. Zhang, D. Jiang, H. Cheng, LncRNA CASC11 improves atherosclerosis by downregulating IL-9 and regulating vascular smooth muscle cell apoptosis and proliferation, Biosci. Biotechnol. Biochem. 83 (2019) 1284–1288, https://doi.org/10.1080/09168451.2019.1597621.

[88] X. Hao, H. Li, P. Zhang, X. Yu, J. Jiang, S. Chen, Down-regulation of lncRNA Gas5 promotes hypoxia-induced pulmonary arterial smooth muscle cell proliferation by regulating KCNK3 expression, Eur. J. Pharmacol. 889 (2020) 173618, https://doi.org/10.1016/j.ejphar.2020.173618.

[89] H. Liu, X.F. Ma, N. Dong, G.N. Wang, M.X. Qi, J.K. Tan, LncRNA PVT1 inhibits endothelial cells apoptosis in coronary heart disease through regulating MAPK1 expression via miR-532-3p, Acta Cardiol. 1 (2023) 1–9, https://doi.org/10.1080/00015385.2023.2209448.

[90] X. Wang, Q. Li, S. He, J. Bai, C. Ma, L. Zhang, X. Guan, H. Yuan, Y. Li, X. Zhu, et al., LncRNA FENDRR with m6A RNA methylation regulates hypoxia-induced pulmonary artery endothelial cell pyroptosis by mediating DRP1 DNA methylation, Mol. Med. 28 (2022) 126, https://doi.org/10.1186/s10020-022-00551-z.

[91] Y. Jiang, B. Hei, W. Hao, S. Lin, Y. Wang, X. Liu, X. Meng, Z. Guan, Clinical value of lncRNA SOX2-OT in pulmonary arterial hypertension and its role in pulmonary artery smooth muscle cell proliferation, migration, apoptosis, and inflammatory, Heart Lung 55 (2022) 16–23, https://doi.org/10.1016/j.hrtlng.2022.04.002.

[92] S. Barangi, A.W. Hayes, G. Karimi, The role of lncRNAs/miRNAs/Sirt1 axis in myocardial and cerebral injury, Cell Cycle 22 (2023) 1062–1073, https://doi.org/10.1080/15384101.2023.2172265.

[93] S. Zhang, K. Qu, S. Lyu, D.L. Hoyle, C. Smith, L. Cheng, T. Cheng, J. Shen, Z.Z. Wang, PEAR1 is a potential regulator of early hematopoiesis of human pluripotent stem cells, J. Cell. Physiol. 238 (2023) 179–194, https://doi.org/10.1002/jcp.30924.

[94] R. Caines, A. Cochrane, S. Kelaini, M. Vila-Gonzalez, C. Yang, M. Eleftheriadou, A. Moez, A.W. Stitt, L. Zeng, D.J. Grieve, et al., The RNA-binding protein QKI controls alternative splicing in vascular cells, producing an effective model for therapy, J. Cell Sci. 132 (2019) jcs230276, https://doi.org/10.1242/jcs.230276.

[95] P.W. Hewett, K. Nishi, E.L. Daft, J. Clifford Murray, Selective expression of erg isoforms in human endothelial cells, Int. J. Biochem. Cell Biol. 33 (2001) 347–355, https://doi.org/10.1016/s1357-2725(01)00022-x.

[96] T.P. Pham, D.I. Bink, L. Stanicek, A. van Bergen, E. van Leeuwen, Y. Tran, L. Matic, U. Hedin, I. Wittig, S. Dimmeler, et al., Long non-coding RNA aerrie controls DNA damage repair via YBX1 to maintain endothelial cell function, Front. Cell Dev. Biol. 8 (2021) 619079, https://doi.org/10.3389/fcell.2020.619079.

[97] B.H. Ramsahoye, D. Biniszkiewicz, F. Lyko, V. Clark, A.P. Bird, R. Jaenisch, Non-CpG methylation is prevalent in embryonic stem cells and may be mediated by DNA methyltransferase 3a, Proc. Natl. Acad. Sci. U.S.A. 97 (2000) 5237–5242, https://doi.org/10.1073/pnas.97.10.5237.

[98] H. Ibrahim, P. Reus, A.K. Mundorf, A.L. Grothoff, V. Rudenko, C. Buschhaus, A. Stefanski, N. Berleth, B. Stork, K. Stühler, et al., Phosphorylation of GAPVD1 is regulated by the PER complex and linked to GAPVD1 degradation, Int. J. Mol. Sci. 22 (2021) 3787, https://doi.org/10.3390/ijms22073787.

[99] S.P. Wu, X.R. Dong, J.N. Regan, C. Su, M.W. Majesky, Tbx18 regulates development of the epicardium and coronary vessels, Dev. Biol. 383 (2013) 307–320, https://doi.org/10.1016/j.ydbio.2013.08.019.

[100] E.M.S. Tan, S.D. Siljee, H.D. Brasch, S. Enriquez, S.T. Tan, T. Itinteang, Embryonic stem cell-like subpopulations in venous malformation, Front. Med. 4 (2017) 162, https://doi.org/10.3389/fmed.2017.00162.

[101] J. Sun, Z. Zhao, W. Zhang, Q. Tang, F. Yang, X. Hu, C. Liu, B. Song, B. Zhang, H. Wang, Spalt-Like protein 4 (SALL4) promotes angiogenesis by activating vascular endothelial growth factor A (VEGFA) signaling, Med. Sci. Mon. Int. Med. J. Exp. Clin. Res. 26 (2020) e920851, https://doi.org/10.12659/MSM.920851.

[102] L.D. Jensen, M. Nakamura, L. Bräutigam, X. Li, Y. Liu, N.J. Samani, Y. Cao, VEGF-B-Neuropilin-1 signaling is spatiotemporally indispensable for vascular and neuronal development in zebrafish, Proc. Natl. Acad. Sci. U.S.A. 112 (2015) E5944–E5953, https://doi.org/10.1073/pnas.1510245112.

[103] I.M. Aspalter, E. Gordon, A. Dubrac, A. Ragab, J. Narloch, P. Vizán, I. Geudens, R.T. Collins, C.A. Franco, C.L. Abrahams, et al., Alk1 and Alk5 inhibition by Nrp1 controls vascular sprouting downstream of Notch, Nat. Commun. 6 (2015) 7264, https://doi.org/10.1038/ncomms8264.

[104] E. Bosseboeuf, A. Chikh, A.B. Chaker, T.P. Mitchell, D. Vignaraja, R. Rajendrakumar, R.S. Khambata, T.D. Nightingale, J.C. Mason, A.M. Randi, et al., Neuropilin-1 interacts with VE-cadherin and TGFBR2 to stabilize adherens junctions and prevent activation of endothelium under flow, Sci. Signal. 16 (2023) eabo4863, https://doi.org/10.1126/scisignal.abo4863.

[105] N. Kofler, M. Simons, The expanding role of neuropilin: regulation of transforming growth factor-β and platelet-derived growth factor signaling in the vasculature, Curr. Opin. Hematol. 23 (2016) 260–267, https://doi.org/10.1097/MOH.0000000000000233.

[106] C. Scimone, L. Donato, S. Alibrandi, T. Esposito, C. Alafaci, R. D'Angelo, A. Sidoti, Transcriptome analysis provides new molecular signatures in sporadic Cerebral Cavernous Malformation endothelial cells, Biochim. Biophys. Acta, Mol. Basis Dis. 1866 (2020) 165956, https://doi.org/10.1016/j.bbadis.2020.165956.
[107] A.M. Bolger, M. Lohse, B. Usadel, Trimmomatic: a flexible trimmer for Illumina sequence data, Bioinformatics 30 (2014) 2114–2120, https://doi.org/10.1093/bioinformatics/btu170.
[108] B.S. Pedersen, K. Eyring, S. De, I.V. Yang, D.A. Schwartz, Fast and accurate alignment of long bisulfite-seq reads, arXiv 1401 (2014) 1129, https://doi.org/10.48550/arXiv.1401.1129.
[109] F. Jühling, H. Kretzmer, S.H. Bernhart, C. Otto, P.F. Stadler, S. Hoffmann, metilene: fast and sensitive calling of differentially methylated regions from bisulfite sequencing data, Genome Res. 26 (2015) 256–262, https://doi.org/10.1101/gr.196394.115.
[110] P. Fonseka, M. Pathan, S.V. Chitti, T. Kang, S. Mathivanan, FunRich enables enrichment analysis of OMICs datasets, J. Mol. Biol. 433 (2021) 166747, https://doi.org/10.1016/j.jmb.2020.166747.
[111] J. Kang, Q. Tang, J. He, L. Li, N. Yang, S. Yu, M. Wang, Y. Zhang, J. Lin, T. Cui, et al., RNAInter v4.0: RNA interactome repository with redefined confidence scoring system and improved accessibility, Nucleic Acids Res. 50 (2022) D326–D332, https://doi.org/10.1093/nar/gkab997.
[112] W.J. Kent, C.W. Sugnet, T.S. Furey, K.M. Roskin, T.H. Pringle, A.M. Zahler, D. Haussler, The human genome browser at UCSC, Genome Res. 12 (2002) 996–1006, https://doi.org/10.1101/gr.229102.